Journal of Thermal Analysis and Calorimetry (2026) 151:6011–6035
https://doi.org/10.1007/s10973-026-15354-1

Experimental and modeling insights into excess molar enthalpy of alcohol–additive ternary mixtures at 298.15 and 313.15 K

Khaoula Samadi[1,3] · Mohamed Lifi[2] · Raúl Briones-Llorente[2] · Fernando Aguilar[3] · Fatima Ezzahrae M'hamdi Alaoui[1]

Received: 6 September 2025 / Accepted: 17 January 2026 / Published online: 6 March 2026

Abstract

The increasing demand for cleaner energy carriers has intensified interest in liquid fuel blends containing oxygenated compounds such as alcohols and glycol ethers. These additives improve combustion efficiency and reduce environmental impact. In this work, excess molar enthalpies were determined for a binary mixtures (ethanol + 1-propanol; diethylene glycol monoethyl ether + 1-propanol; and ethylene glycol monophenyl ether + ethanol) as well as for four ternary mixtures: diethylene glycol monomethyl ether (1) + 1-propanol (2) + ethanol (3), diethylene glycol monoethyl ether (1) + 1-propanol (2) + ethanol (3), ethylene glycol monomethyl ether (1) + 1-propanol (2) + ethanol (3), and ethylene glycol monophenyl ether (1) + 1-propanol (2) + ethanol (3). Measurements were obtained with a quasi-isothermal flow calorimeter at 298.15 K and 313.15 K under 0.1 MPa, conditions representative of typical industrial applications. The experimental data were then correlated using the Redlich–Kister equation for the binary system and the NRTL, UNIQUAC, and modified UNIFAC (Dortmund) models for the ternary systems, enabling evaluation of both mixture behavior and model accuracy. The findings expand the thermodynamic database for alcohol- and glycol ether-based blends and provide benchmarks for simulation and design in energy and petrochemical processes.

Keywords Excess molar enthalpy · Ternary mixtures · Oxygenated additives · Redlich–Kister correlation · Local composition models

Introduction

Many glycol ethers, including diethylene glycol monoethyl ether, diethylene glycol monomethyl ether, ethylene glycol monomethyl ether, and ethylene glycol monophenyl ether, are solvents of considerable industrial importance [1]. Their molecular structure featuring both ether and hydroxyl functionalities allows for notable solvation capabilities, particularly in systems where hydrogen bonding and dipole–dipole interactions play a significant role [2]. These compounds are commonly incorporated into formulations ranging from surface coatings to cleaning agents, owing to their ability to interact with both polar and nonpolar substances.

1-Propanol is a short-chain aliphatic alcohol widely used as a solvent and intermediate in chemical synthesis [3]. Its structure, consisting of a hydroxyl group attached to a three-carbon backbone, imparts amphiphilic character: The hydroxyl moiety promotes strong hydrogen bonding, while the hydrophobic tail influences dispersion forces and molecular packing. In the pure state, 1-propanol molecules are extensively self-associated through O–H···O interactions, forming a dynamic hydrogen-bonded network. These features make 1-propanol particularly relevant in studies of non-ideal liquid mixtures, as its balance of polar and nonpolar interactions strongly modulates the thermodynamic behavior when combined with other associating solvents such as ethanol or glycol ethers [4].

In mixtures with short-chain alcohols such as ethanol and 1-propanol, glycol ethers contribute to highly non-ideal behavior [5]. The degree of this non-ideality is closely linked to the nature and strength of intermolecular forces present in

✉ Mohamed Lifi
mlifi@ubu.es

1 Energy Laboratory, Faculty of Sciences, Abdelmalek Essaadi University, Tetouan, Morocco

2 Department of Mathematics and Computing, Faculty of Science, University of Burgos, 09001 Burgos, Spain

3 Departamento de Ingeniería Electromecánica, Escuela Politécnica Superior, Universidad de Burgos, Burgos, Spain

the system. One key thermodynamic property used to assess this is the excess molar enthalpy, which reflects the enthalpic deviation from ideal solution behavior and provides insight into energetic interactions during mixing.

When substances capable of hydrogen bonding are combined especially those with multiple donor and acceptor sites, the resulting H_m^E values can exhibit complex, composition-dependent trends. In binary mixtures, H_m^E helps reveal whether mixing is exothermic or endothermic, often correlating with the formation or disruption of hydrogen bonds. However, in ternary systems, such as those involving a glycol ether, ethanol, and 1-propanol, the interaction landscape becomes more intricate. Competitive association between three molecular species may produce synergistic or antagonistic effects, which simple binary models cannot capture.

The experimental determination of excess molar enthalpies in such ternary systems is essential for accurately describing their mixing behavior [6]. These data are indispensable for calibrating and validating thermodynamic models such as NRTL, UNIQUAC, and group-contribution approaches like UNIFAC. Without accurate experimental values, such models may fail to reflect the real behavior of associating mixtures.

Furthermore, understanding the enthalpic effects in systems containing glycol ethers and alcohols is increasingly relevant in the context of sustainable solvent design [7]. With growing interest in replacing traditional volatile organic compounds with lower-toxicity alternatives, characterizing these systems thermodynamically supports efforts in formulation science, process engineering, and green chemistry.

Beyond their role as solvents, glycol ethers and short-chain alcohols are increasingly studied as oxygenated additives in fuel formulations. Their incorporation enhances combustion efficiency, reduces pollutant emissions, and improves miscibility in multicomponent blends [8]. Thermodynamic characterization of such mixtures thus supports the design of cleaner, high-performance fuels.

In thermodynamic and fuel-related studies, 298.15 K (25 °C) is commonly adopted as the standard reference temperature [9]. This value reflects typical ambient conditions and is widely used to characterize fuel properties as they enter engines, and during handling, blending, and storage operations. Employing data gathered at this temperature is essential to ensure consistency across scholarly and engineering sources and is extensively used for populating simulation tools and thermophysical property databases. NIST, for instance, often cites 298.15 K and 1 bar as standard conditions for experimental measurements.

On the other hand, 313.15 K (40 °C) is frequently used to represent fuel temperatures under actual operating scenarios such as within injectors or pipeline segments during engine operation. This temperature is also pertinent to numerous chemical and separation processes, including biodiesel purification, liquid–liquid extraction, and distillation, which commonly operate in the 30–60 °C range. Thus, experimental data at 313.15 K are invaluable for optimizing not only fuel delivery systems, but also broader industrial processes.

Therefore, combining measurements taken at 298.15 K and 313.15 K (with standard atmospheric pressure around 0.1 MPa) is critically important when determining and modeling thermophysical properties of fuels. Datasets spanning these two reference temperatures provide both comparability with literature values and practical relevance to real-world engineering applications.

This work presents a detailed investigation into the excess molar enthalpies of binary and ternary mixtures comprising selected glycol ethers, ethanol, and 1-propanol. The study aims to provide high-quality experimental data to improve the understanding of molecular interactions in multicomponent liquid systems and to support the development of predictive thermodynamic models. Excess molar enthalpies, H_m^E, of binary and ternary mixtures containing (*i*) ethanol + 1-propanol, (*ii*) diethylene glycol monoethyl ether + 1-propanol, (*iii*) ethylene glycol monophenyl ether + ethanol, (*iv*) diethylene glycol monomethyl ether (1) + 1-propanol (2) + ethanol (3), (*v*) diethylene glycol monoethyl ether (1) + 1-propanol (2) + ethanol (3), (*vi*) ethylene glycol monomethyl ether (1) + 1-propanol (2) + ethanol (3), and (*vii*) ethylene glycol monophenyl ether (1) + 1-propanol (2) + ethanol (3) are determined in this work at 298.15 and 313.15 K and at 0.1 MPa. H_m^E was generated using a quasi-isothermal calorimeter for all the studied binary and ternary mixtures. All these mixtures reveal endothermic behavior at all temperatures. Moreover, the experimental data for excess molar enthalpy, H_m^E, were correlated using the modified Redlich–Kister equation [10], the NRTL [11], the modified UNIFAC (Dortmund) [12], and the UNIQUAC [13] models.

Chemicals

The components investigated in this study are diethylene glycol monomethyl ether (DEGME) ($C_5H_{12}O_3$); diethylene glycol monoethyl ether (DEGEE) (22EEE) $\left(C_6H_{14}O_3\right)$; ethylene glycol monomethyl ether (EGME) ($C_3H_8O_2$); ethylene glycol monophenyl ether (EGPhE) ($C_8H_{10}O_2$); 1-propanol (1-PrOH) (C_3H_8O); and ethanol (C_2H_6O). These compounds were used to prepare four ternary mixtures in which each glycol ether (DEGME, DEGEE, EGME, or EGPhE) was combined with 1-PrOH and ethanol. Relevant physicochemical data of the pure substances, including molecular formula, molar mass, density, mole fraction purity, water content, and CAS number, are listed in Table 1. All chemicals were

supplied with a mass fraction purity higher than 99%, and no further purification was required prior to use.

Materials and methods

A quasi-isothermal calorimeter was employed to determine the H_m^E of the investigated binary and ternary mixtures. A schematic representation of the experimental setup is given in Fig. 1. Experiments were carried out at 298.15 and 313.15 K. The mole fractions (x_i) of the mixture components were obtained from the measured flow rates of the liquids, together with their molecular masses and densities. The associated standard uncertainty was estimated as $u(x)=0.0008$. Table 1 reports the densities, ρ, of the pure compounds at the delivery temperatures [14–18]. The dependence of H_m^E on composition was studied by preparing mixtures of different mole fractions. The excess molar enthalpy was obtained from the relation:

$$H_m^E = \frac{Q_{mixture}}{\dot{n}_{mixture}} \quad (1)$$

where $Q_{mixture}$ is the measured heat effect of mixing and $\dot{n}_{mixture}$ is the total molar flow rate of the solution. Thus, H_m^E for each composition was determined by dividing the thermal power released in the mixing cell by the molar flow rate

Table 1 Purity and chemical data of used liquids

Compound	Formula	Molar mass /g mol^{-1}	Density[a] /g cm^{-3}		State mole fraction purity[f]/ mol%	Water content[g]/ mass%	CAS number
			298.15 K	313.15 K			
DEGME*	$C_5H_{12}O_3$	120.15	1.0147[a]	1.0014[a]	> 99.0	≤ 0.03	111-77-3
DEGEE*	$C_6H_{14}O_3$	134.18	0.9852[b]	0.9718[b]	> 99.0	≤ 0.03	111-90-0
EGME*	$C_3H_8O_2$	76.09	0.9598[c]	0.9460[c]	> 99.8	≤ 0.01	109-86-4
EGPhE*	$C_8H_{10}O_2$	138.18	1.1030[d]	1.0900[d]	> 99.0	≤ 0.02	122-99-6
1-PrOH*	C_3H_8O	60.1	0.8000[d]	0.7880[d]	> 99.9	≤ 0.02	71-23-8
Ethanol	C_2H_6O	46.07	0.7852[e]	0.7916[e]	> 99.8	≤ 0.02	64-17-5

[a]Lifi et al. [16]; [b]Lifi et al. [17]; [c]Lifi et al. [15]; [d]Makhlouf et al. [14]; [e]Lifi et al.[18]

[f]Determined by gas chromatography (GC) by the supplier

[g]Water content is given in mass fractions and measured by Karl Fischer titration

*DEGME: diethylene glycol monomethyl ether; DEGEE: diethylene glycol monoethyl ether; EGME: ethylene glycol monomethyl ether; EGPhE: ethylene glycol monophenyl ether; and 1-PrOH: 1-propanol

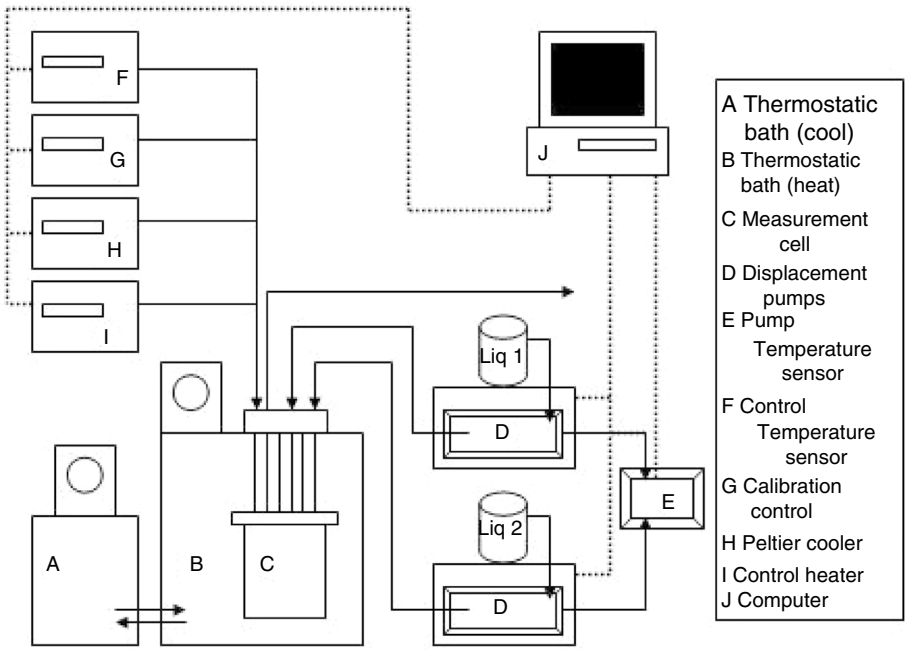

Fig. 1 Quasi-isothermal flow calorimeter. Schematic diagram

of the mixture. In binary systems, both streams correspond to the pure liquids, whereas in ternary mixtures, one stream is a pure liquid and the other is a premixed binary solution. The expanded relative uncertainty associated with the excess molar enthalpy measurements was evaluated as ($k=2$) $Ur(H_m^E)=1\%$. An in-depth explanation and validation of the experimental procedure can be found in our earlier work [19]. The uncertainty budget of H_m^E, calculated following the EA-4/02 guidelines [20], is summarized in Table 2.

Equations and models

Modified Redlich–Kister equation

Binary mixture results were analyzed using the R–K equation [10], expressed as:

$$H_m^E = \frac{x(1-x)\sum_{i-1}^{n} A_i(2x-1)^{i-1}}{1+A_0(2x-1)} \quad (2)$$

where A_i coefficients were obtained by the unweighted least-squares method of the experimental data obtained in this work. The optimal number of coefficients was determined using the F test [21].

NRTL model

Excess molar enthalpies were also correlated using the non-random two-liquid (NRTL) model [11]. The general expression is given by:

$$H_m^E = -RT\sum_{i=1}^{n} x_i\eta_i \quad (3)$$

where x_i is the fractional composition of compound i and η_i is defined as:

$$\eta_i = \frac{\sum_{k=1}^{p} x_k\tau_{ki}G_{ki}\left[\alpha\left(\tau_{ki}-\left(\sum_{n=1}^{p} x_n\tau_nG_n/\sum_{l=1}^{n} x_lG_{li}\right)\right)-1\right]}{\sum_{l=1}^{n} x_lG_{li}} \quad (4)$$

where α accounts for non-uniformity of molecular forces, thereby enhancing the accuracy of phase equilibrium predictions. In the NRTL framework, G_{ji} is expressed as $G_{ji}=\exp(-\alpha\tau_{ij})$, where $\tau_{ij}=(g_{ij}-g_{ii})/RT$, with g_{ij} representing the strength of intermolecular forces expressed as interaction energy between i and j. All NRTL binary interaction parameters were obtained by fitting the present experimental data, making this model correlative rather than predictive in the current study. The NRTL model is particularly well suited for systems dominated by strong hydrogen bonding.

UNIQUAC model

The UNIQUAC model [13] was employed to describe the correlation of the excess molar enthalpies, H_m^E. Its mathematical form is given as:

$$H_m^E = \sum_{i=1}^{n} q_ix_i\frac{\sum_{j=1}^{n}\vartheta_j\Delta u_{ji}\tau_{ji}}{\sum_{j=1}^{n}\vartheta_j\tau_{ij}} \quad (5)$$

where $\vartheta_j=\frac{q_ix_i}{\sum_j q_ix_i}$ and q_i represents the molecular surface area, obtained by adding the contributions of the functional groups present in the molecule. The UNIQUAC binary interaction parameters Δu_{ij} were determined by regression of the experimental excess enthalpy data measured in this work.

Table 2 Uncertainty budget for excess enthalpy using EA-4/02 [20]*

		Units	Estimate	Divisor	Uncertainty value
$U(Q_{mixture})$	Resolution	W	$4\cdot10^{-6}$	$2\sqrt{3}$	$1.15\cdot10^{-6}$
$u(Q_{mixture})$	Repeatability		$4\cdot10^{-6}$	1	$4\cdot10^{-6}$
$u(Q_{mixture})$	Nonlinearity		$1.2\cdot10^{-4}$	1	$1.2\cdot10^{-4}$
$U(\dot{V}_1)$	Accuracy	$cm^3\cdot s^{-1}$	$2.5\cdot10^{-5}$	2	$1.25\cdot10^{-5}$
	Resolution		$1.7\cdot10^{-5}$	$2\sqrt{3}$	$7.22\cdot10^{-6}$
$U(\dot{V}_2)$	Accuracy	$cm^3\cdot s^{-1}$	$2.5\cdot10^{-5}$	2	$1.25\cdot10^{-5}$
	Resolution		$1.7\cdot10^{-5}$	$2\sqrt{3}$	$7.22\cdot10^{-6}$
$u(T)$	Stability	K	$1\cdot10^{-2}$	1	0.01
$u(H_m^E)$	$H_m^E=400$	$J\cdot mol^{-1}$	N/A	$k=1$	0.9
$U(H_m^E)$		$J\cdot mol^{-1}$	N/A	$k=2$	1.8
$U_r(H_m^E)$		$J\cdot mol^{-1}/J\cdot mol^{-1}$	N/A	$k=2$	$5\cdot10^{-3}$

*$Q_{mixture}$: heat of mixing; $\dot{V}_1$ and $\dot{V}_2$: flows of pure components 1 and 2 driven by isocratic pumps; T: temperature; H_m^E: excess molar enthalpy; and x: mole fraction

Note that u represents the standard uncertainty, U is the expanded uncertainty with a stated coverage factor of $k=2$, and U_r is the relative expanded uncertainty with a coverage factor stated in column "Divisor"

Modified UNIFAC (Dortmund) model

The DM-UNIFAC group-contribution method was used in its predictive form to estimate activity coefficients for the studied systems. No parameters were adjusted in the present work. All group interaction parameters and structural constants were taken from the DM-UNIFAC parameter tables reported in the literature [12, 22].

In the UNIFAC framework, the activity coefficient of component i is expressed as the sum of combinatorial and residual contributions:

$$\ln \gamma_i = \ln \gamma_i^C + \ln \gamma_i^R \tag{6}$$

The residual contribution, which accounts for energetic interactions between functional groups, is given by:

$$\ln \gamma_i^R = \sum_K^{\text{groups}} \upsilon_K^{(i)} \left[\ln \Gamma_K - \ln \Gamma_K^{(i)} \right] \tag{7}$$

where γ_i^R denotes the number of functional groups of type k in molecule i. Γ_K denotes the residual activity coefficient of group k in the defined solution at the given temperature T, while $\Gamma_K^{(i)}$ represents the residual activity coefficient of the corresponding functional group in a reference solution defined by the pure component at the studied temperature.

The group interaction parameter ψ_{nm} in the modified UNIFAC (Dortmund) model is temperature dependent and is expressed as:

$$\psi_{nm} = exp\left(-\frac{a_{nm} + b_{nm}T + c_{nm}T^2}{T} \right) \tag{8}$$

The parameters a_{nm}, b_{nm}, and c_{nm} were taken from the standard Dortmund UNIFAC parameter database and were not fitted to the present experimental data.

The Γ_K of group k in the mixture is calculated as:

$$\ln \Gamma_K = Q_K \left[1 - \ln \left(\sum_m \Theta_m \psi_{mk} \right) - \sum_m \frac{(\Theta_m \psi_{km})}{\sum_n \Theta_n \psi_{nm}} \right] \tag{9}$$

An analogous expression applies for $\ln \Gamma_k^{(i)}$, which corresponds to a reference solution consisting of pure component i. The group surface area fraction Θ_m is defined as:

$$\Theta_m = \frac{Q_m X_m}{\sum_n Q_n X_n} \tag{10}$$

where X_m is the mole fraction of group m in the mixture and Q_m is the group surface area parameter.

Based on the temperature dependence of the residual term, the excess molar enthalpy is obtained as:

$$H_m^E = -RT^2 \sum_i \sum_k x_i \upsilon_K^{(i)} \left[\left(\frac{\partial \ln \Gamma_K}{\partial T} \right)_{p,x} - \left(\frac{\partial \ln \Gamma_K^{(i)}}{\partial T} \right)_{p,x} \right] \tag{11}$$

where $\upsilon_K^{(i)}$ is the number of groups of type k in molecule i, R is the universal gas constant, and T is the absolute temperature.

Accuracy test

To evaluate the accuracy of the correlations, the following statistical metrics were employed: absolute average deviation (AAD), root-mean-square error (RMSE), and maximum deviation (Max ($|\Delta H_m^E|$)).

$$AAD = \frac{100}{N} \sum_{i=1}^{N} \left| \frac{H_{m,exp}^E - H_{m,calc}^E}{H_{exp}^E} \right| \tag{12}$$

$$rms = \left[\frac{\sum_{i=1}^{N} \left(H_{m,exp}^E - H_{m,calc}^E \right)^2}{N - n_{par}} \right]^{1/2}. \tag{13}$$

$$\text{Max} \left| \Delta H_m^E \right| = \text{Max} \left| H_{m,exp}^E - H_{m,calc}^E \right| \tag{14}$$

$H_{m,exp}^E$, $H_{m,calc}^E$, N, and n_{par} are, respectively, the experimental and calculated data of H_m^E, the number of experimental points, and the number of adjustable parameters used in each model (Table 3).

Results and discussion

Excess molar enthalpies, H_m^E, were determined for the binary systems: ethanol + 1-PrOH, DEGEE + 1-PrOH, and EGPhE + ethanol as well as for several ternary mixtures including glycol ethers with ethanol and 1-propanol, namely x_1 DEGME + x_2 1-PrOH + (1-x_1-x_2) ethanol, x_1 DEGEE + x_2 1-PrOH + (1-x_1-x_2) ethanol, x_1 EGME + x_2 1-PrOH + (1-x_1 -x_2) ethanol, and x_1 EGPhE + x_2 1-PrOH + (1-x_1-x_2) ethanol at 298.15 K and 313.15 K. In addition, H_m^E data of the binary mixtures containing, respectively, DEGME + ethanol; DEGEE + ethanol; EGME + ethanol; DEGME + 1-PrOH; EGME + 1-PrOH; and EGPhE + 1-PrOH at (298.15 and 313.15) K have been documented in prior works [14, 15, 18, 23]. A summary of the present measurements is reported in Table 4, Tables S1, and S2 (see Supplementary Materials), with the corresponding concentration dependences illustrated in Figs. 2–6. Comparisons between experimental and fitted excess molar enthalpy curves obtained using

Table 3 Sets of parameters needed for the graphical representation of excess molar enthalpy, H_m^E, by Redlich–Kister equation, NRTL, and UNIQUAC models, for studied binary mixture ethanol (1) +1-PrOH (2), DEGEE (1) + 1-PrOH (2), and EGPhE (1) + ethanol (2) at (298.15 and 313.15) K and at $P = 0.1$ MPa

Binary system[a] at 298.15 K								
Redlich–Kister			NRTL			UNIQUAC		
Ethanol (1) +1-PrOH (2)								
A_0	J·mol^{-1}	− 0.2705	τ_{12}	J·mol^{-1}	0.1199	Δu_{12}	J·mol^{-1}	356.9
A_1		90.9	τ_{21}		− 0.0771	Δu_{21}		− 296.6
A_2		− 11.7	α_{12}		0.30			
A_3		− 3.33						
MAD (%)		1.29	MAD (%)		4.49	MAD (%)		3.29
rms ΔH_m^E/J·mol^{-1}		0.2	*rms* ΔH_m^E/J·mol^{-1}		0.5	*rms* ΔH_m^E/J·mol^{-1}		0.4
Max $\lvert\Delta H_m^E\rvert$/J·mol^{-1}		0.4	Max $\lvert\Delta H_m^E\rvert$/J·mol^{-1}		0.9	Max $\lvert\Delta H_m^E\rvert$/J·mol^{-1}		0.8
DEGEE (1) +1-PrOH (2)								
A_0	J·mol^{-1}	0.4216	τ_{12}	J·mol^{-1}	0.1125	Δu_{12}	J·mol^{-1}	948.2
A_1		2060.5	τ_{21}		1.0550	Δu_{21}		− 134.2
A_2		280.7	α_{12}		0.30			
A_3		− 37.7						
MAD (%)		0.31	MAD (%)		0.81	MAD (%)		0.65
rms ΔH_m^E/J·mol^{-1}		0.8	*rms* ΔH_m^E/J·mol^{-1}		3.04	*rms* ΔH_m^E/J·mol^{-1}		2.40
Max $\lvert\Delta H_m^E\rvert$/J·mol^{-1}		1.0	Max $\lvert\Delta H_m^E\rvert$/J·mol^{-1}		5.40	Max $\lvert\Delta H_m^E\rvert$/J·mol^{-1}		3.99
EGPhE (1) + ethanol (2)								
A_0	J·mol^{-1}	0.2077	τ_{12}	J·mol^{-1}	567.0000	Δu_{12}	J·mol^{-1}	26815.0
A_1		1354.1	τ_{21}		0.7259	Δu_{21}		323.9
A_2		− 88.1	α_{12}		0.30			
A_3		365.4						
MAD (%)		0.34	MAD (%)		5.67	MAD (%)		4.94
rms ΔH_m^E/J·mol^{-1}		0.90	*rms* ΔH_m^E/J·mol^{-1}		12.92	*rms* ΔH_m^E/J·mol^{-1}		11.80
Max $\lvert\Delta H_m^E\rvert$/J·mol^{-1}		1.07	Max $\lvert\Delta H_m^E\rvert$/J·mol^{-1}		25.62	Max $\lvert\Delta H_m^E\rvert$/J·mol^{-1}		24.05
Binary system[a] at 313.15 K								
Redlich–Kister			NRTL			UNIQUAC		
Ethanol (1) +1-PrOH (2)								
A_0	J·mol^{-1}	− 1.0504	τ_{12}	J·mol^{-1}	0.2205	Δu_{12}	J·mol^{-1}	− 337.8
A_1		77.9	τ_{21}		− 0.1675	Δu_{21}		411.8
A_2		− 68.7	α_{12}		0.30			
A_3		− 13.29						
MAD (%)		2.28	MAD (%)		2.70	MAD (%)		2.98
rms ΔH_m^E/J·mol^{-1}		0.3	*rms* ΔH_m^E/J·mol^{-1}		0.2	*rms* ΔH_m^E/J·mol^{-1}		0.3
Max $\lvert\Delta H_m^E\rvert$/J·mol^{-1}		0.5	Max $\lvert\Delta H_m^E\rvert$/J·mol^{-1}		0.5	Max $\lvert\Delta H_m^E\rvert$/J·mol^{-1}		0.6
DEGEE (1) +1-PrOH (2)								
A_0	J·mol^{-1}	0.0721	τ_{12}	J·mol^{-1}	0.1104	Δu_{12}	J·mol^{-1}	323.8
A_1		2181.7	τ_{21}		1.0690	Δu_{21}		188.4
A_2		− 508.1	α_{12}		0.30			
A_3		130.5274						
MAD (%)		0.20	MAD (%)		0.20	MAD (%)		0.43
rms ΔH_m^E/J·mol^{-1}		0.7	*rms* ΔH_m^E/J·mol^{-1}		0.7	*rms* ΔH_m^E/J·mol^{-1}		1.1
Max $\lvert\Delta H_m^E\rvert$/J·mol^{-1}		1.0	Max $\lvert\Delta H_m^E\rvert$/J·mol^{-1}		1.2	Max $\lvert\Delta H_m^E\rvert$/J·mol^{-1}		2.5
EGPhE (1) + ethanol (2)								
A_0	J·mol^{-1}	0.1338	τ_{12}	J·mol^{-1}	0.0846	Δu_{12}	J·mol^{-1}	54.3
A_1		1805.0	τ_{21}		0.8253	Δu_{21}		369.3

Table 3 (continued)

Binary system[a] at 313.15 K					
Redlich–Kister		NRTL		UNIQUAC	
Ethanol (1) +1-PrOH (2)					
A_2	− 172.3	α_{12}	0.30		
A_3	266.3				
MAD (%)	0.20	MAD (%)	3.00	MAD (%)	2.77
rms ΔH_m^E/J·mol^{-1}	0.70	*rms* ΔH_m^E/J·mol^{-1}	7.30	*rms* ΔH_m^E/J·mol^{-1}	6.74
Max $\lvert\Delta H_m^E\rvert$/J·mol^{-1}	1.14	Max $\lvert\Delta H_m^E\rvert$/J·mol^{-1}	11.74	Max $\lvert\Delta H_m^E\rvert$/J·mol^{-1}	10.61

[a]DEGEE: diethylene glycol monoethyl ether; EGPhE: ethylene glycol monophenyl ether; and 1-PrOH: 1-propanol

Eq. (16), Eq. (18), NRTL, and UNIQUAC models are further presented in Figs. 7 and 8 for a fixed composition ratio $x_2/x_3 = 0.25$.

The interaction parameters required to reproduce the H_m^E data using the modified R–K equation, NRTL, and UNIQUAC models are provided in Tables 3, 5, and 6. Information regarding the structural groups of the studied compounds, including their van der Waals volumes R_K and surface area parameters Q_K, as well as the specific group interaction coefficients, is presented in Tables 7 and 9. Finally, molecular structures and their subgroup decompositions are shown in Table 8.

- Ethanol + 1-PrOH

The H_m^E of the binary mixture ethanol (1) + 1-propanol (2) exhibit endothermic behavior ($H_m^E > 0$) at both studied temperatures. As shown in Fig. 2 (a), the H_m^E curves are skewed, with maximum values of approximately 22.7 J.mol^{-1} at 298.15 K occurring near $x_1 \approx 0.5498$ and 19.6 J.mol^{-1} at 313.15 K which appear near $x_1 \approx 0.55$. The positive values of H_m^E arise from the partial disruption of hydrogen bonds present in the pure alcohols when they are mixed. In pure ethanol and pure 1-propanol, molecules are strongly self-associated through extensive O–H···O hydrogen-bond networks. Upon mixing, these networks are rearranged into new ethanol–propanol associations, which are weaker and less energetically favorable. The energy required to break the stronger self-associations exceeds the stabilization gained by forming mixed hydrogen bonds, leading to a net endothermic effect (Table 9).

From a molecular perspective, the asymmetry of the H_m^E curves is related to differences in molecular size, shape, and polarity between ethanol and 1-propanol. Ethanol is shorter and more polar, whereas 1-propanol has a larger hydrophobic tail, which introduces steric hindrance and reduces the strength and number of hydrogen bonds per molecule. This mismatch in molecular packing and hydrogen-bonding capacity explains the skewness of the enthalpy curves and the maximum near equimolar composition, where the disruption of self-association is most pronounced.

Concerning model performance, the R–K equation reproduces the experimental data with the lowest AAD values (1.29% at 298.15 K and 2.28% at 313.15 K), confirming its empirical accuracy. The NRTL model also performs well, since it accounts for non-random mixing and local interactions, reflecting the heterogeneous molecular environments in the mixture. UNIQUAC provides a fair description by including both combinatorial effects (size/shape of molecules) and residual energetic contributions, but it underestimates enthalpic deviations at high ethanol content, where directional hydrogen bonding is dominant.

The UNIFAC model exhibits a temperature-dependent predictive ability. At 298.15 K, it fails to capture the magnitude of H_m^E, since its group-contribution scheme neglects explicit hydrogen bonding, which dominates the thermodynamics at lower temperature. At 313.15 K, however, hydrogen-bond interactions are weakened, and dispersive, steric, and group–group interactions become more significant. As a result, UNIFAC achieves a much better agreement with experimental data at the higher temperature.

When comparing our results with the literature [24], a good consistency is found at 298.15 K. However, it should be noted that the pressure conditions reported in the reference are not explicitly specified, which may slightly affect the comparison. Moreover, the calorimetric technique used in that work differs from the quasi-isothermal method employed in the present study. These differences in experimental conditions and methodology must be taken into account when evaluating the agreement between datasets. At 313.15 K, no data are available in the literature for this system, making our measurements an original and valuable contribution to the thermodynamic characterization and molecular understanding of binary alcohol mixtures.

Table 4 Excess molar enthalpy, H_m^E, measured data of studied binary mixture x_1 ethanol + $(1 - x_1)$ 1-PrOH, x_1 DEGEE + $(1 - x_1)$ 1-PrOH, and x_1 EGPhE + $(1 - x_1)$ ethanol at T = 298.15 and 313.15 K and at P = 0.1 MPa[a]

x_1/mol	H_m^E/J·mol^{-1}	x_1/mol	H_m^E/J·mol^{-1}	x_1/mol	H_m^E/J·mol^{-1}	x_1/mol	H_m^E/J·mol^{-1}
x_1 ethanol + $(1 - x_1)$ 1-PrOH[b]							
At 298.15 K							
0.0506	3.5	0.3006	18.2	0.5498	22.7	0.7994	15.7
0.1001	6.9	0.3495	19.8	0.6001	22.4	0.8498	12.8
0.1503	10.5	0.4002	21.3	0.6491	21.6	0.9001	9.3
0.1993	13.4	0.4497	22.2	0.6997	20.2	0.9502	4.9
0.2505	16.0	0.4997	22.6	0.7502	18.3		
At 313.15 K							
0.0506	2.7	0.3006	15.3	0.5500	19.6	0.7994	13.7
0.1001	6.6	0.3495	17.0	0.6001	19.5	0.8498	11.1
0.1503	9.0	0.4003	18.0	0.6492	18.7	0.9001	8.3
0.1993	11.1	0.4499	19.0	0.6997	17.7	0.9502	4.6
0.2505	13.0	0.4998	19.3	0.7502	15.8		
x_1 DEGEE + $(1 - x_1)$ 1-PrOH[b]							
At 298.15 K							
0.0499	134.6	0.2994	490.2	0.5489	496.0	0.7991	285.0
0.0995	245.4	0.3498	513.4	0.5997	468.5	0.8498	221.1
0.1501	334.5	0.3994	524.3	0.6500	432.6	0.9007	150.2
0.1993	402.0	0.4493	524.8	0.6991	390.9	0.9492	77.8
0.2500	454.7	0.4991	515.5	0.7488	340.4		
At 313.15 K							
0.0499	137.5	0.2994	519.7	0.5487	524.0	0.7991	296.6
0.0994	254.1	0.3497	545.3	0.5995	493.9	0.8498	230.0
0.1500	349.7	0.3993	556.6	0.6498	454.4	0.9007	156.3
0.1993	422.8	0.4491	557.2	0.6990	409.6	0.9492	82.1
0.2499	481.0	0.4990	545.5	0.7488	356.5		
x_1 EGPhE + $(1 - x_1)$ ethanol							
At 298.15 K							
0.0502	99.0	0.2993	331.4	0.5497	327.2	0.8007	203.1
0.0997	178.2	0.3494	342.4	0.5989	311.9	0.8510	163.0
0.1494	237.7	0.3997	346.2	0.6496	292.2	0.8989	117.5
0.1993	281.7	0.4495	344.4	0.6998	267.9	0.9495	62.8
0.2498	312.6	0.5003	338.4	0.7487	239.1		
At 313.15 K							
0.0502	118.6	0.2994	424.3	0.5498	438.2	0.8008	266.1
0.0998	212.4	0.3495	445.8	0.5989	416.0	0.8510	210.6
0.1495	288.8	0.3997	455.9	0.6498	387.9	0.8989	150.6
0.1994	347.8	0.4497	458.5	0.6998	355.5	0.9495	80.5
0.2499	393.0	0.5003	451.7	0.7488	313.7		

[a]Standard uncertainties of pressure p, temperature T, and mole fraction x are as follows: $u(p) = 0.01$ MPa, $u(T) = 0.05$ K, $u(x) = 0.0008$. The relative expanded uncertainty ($k = 2$) is $U_r(H_m^E) = 0.01$ for excess molar enthalpy

[b]x_1 is the mole fraction of ethanol; DEGEE or EGPhE

- DEGEE + 1-PrOH

The H_m^E values of the binary mixture DEGEE (1) + 1-PrOH (2) are positive over the entire composition range at both 298.15 and 313.15 K, confirming an endothermic mixing process. As illustrated in Fig. 2 (b), the excess molar enthalpy curves display a clear maximum near intermediate mole fractions, with higher values observed at 313.15 K compared to 298.15 K, indicating that the enthalpic cost of disrupting hydrogen-bond networks increases with temperature. The maxima reach approximately 524.8

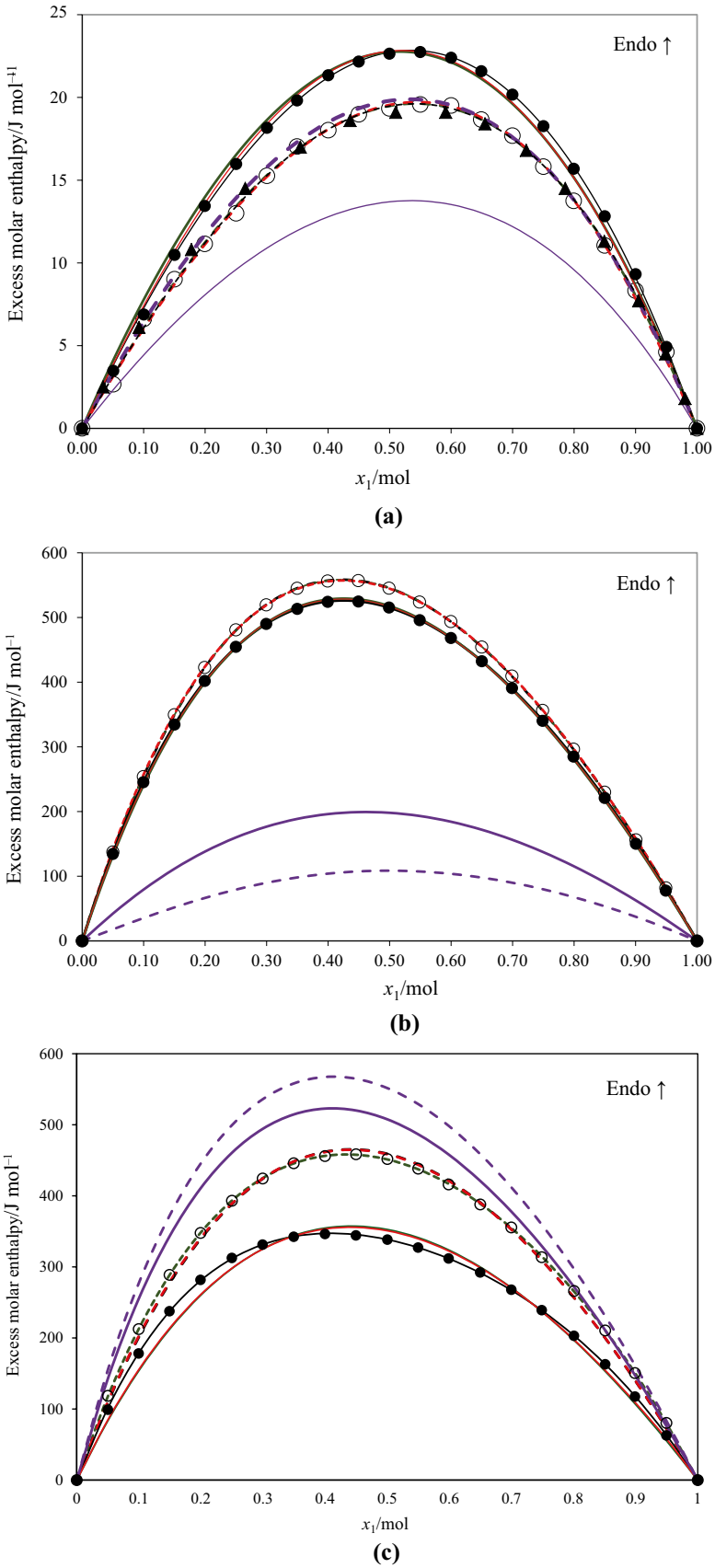

Fig. 2 Excess molar enthalpy H_m^E of **a** ethanol (1) + 1-propanol (2), **b** diethylene glycol monoethyl ether (1) + 1-propanol (2), and (c) ethylene glycol monophenyl ether (1) + ethanol (2). At $T = 298.15$ K: (·), experimental data; (▲), Pflug et al. [24]; (——), calculated values with modified Redlich–Kister equation; (——), calculated values with NRTL model; (——), calculated values with UNIQUAC model; and (——), calculated values with UNIFAC model. At $T = 313.15$ K: (○), experimental data; (----), calculated values with modified Redlich–Kister equation; (----), calculated values with NRTL model; (----), calculated values with UNIQUAC model; and (----), calculated values with UNIFAC model

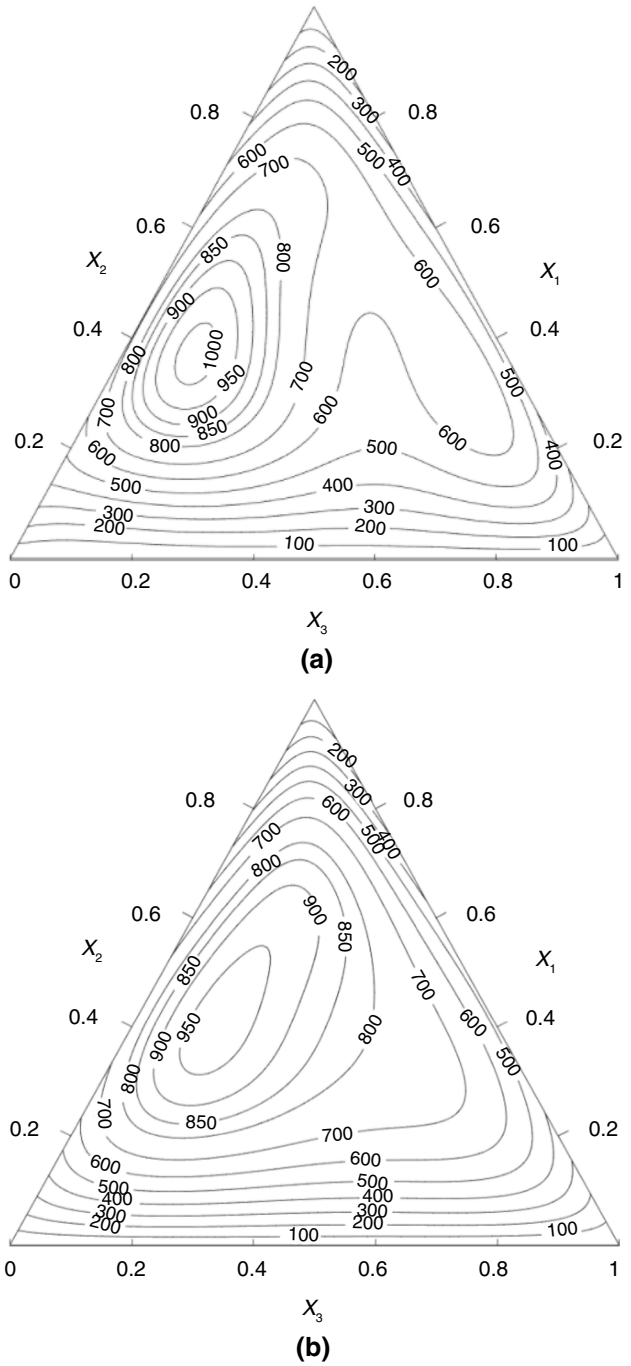

Fig. 3 Contours for constant values of H^{E}_{123} for ternary mixture diethylene glycol monomethyl ether (1) + 1-propanol (2) + ethanol (3), calculated from the representation of the experimental results by Eqs. (17 and 18) using the parameters given in Tables 5 and 6: **a**, at 298.15 K; **b**, at 313.15 K. This figure is plotted using MATLAB Simulink

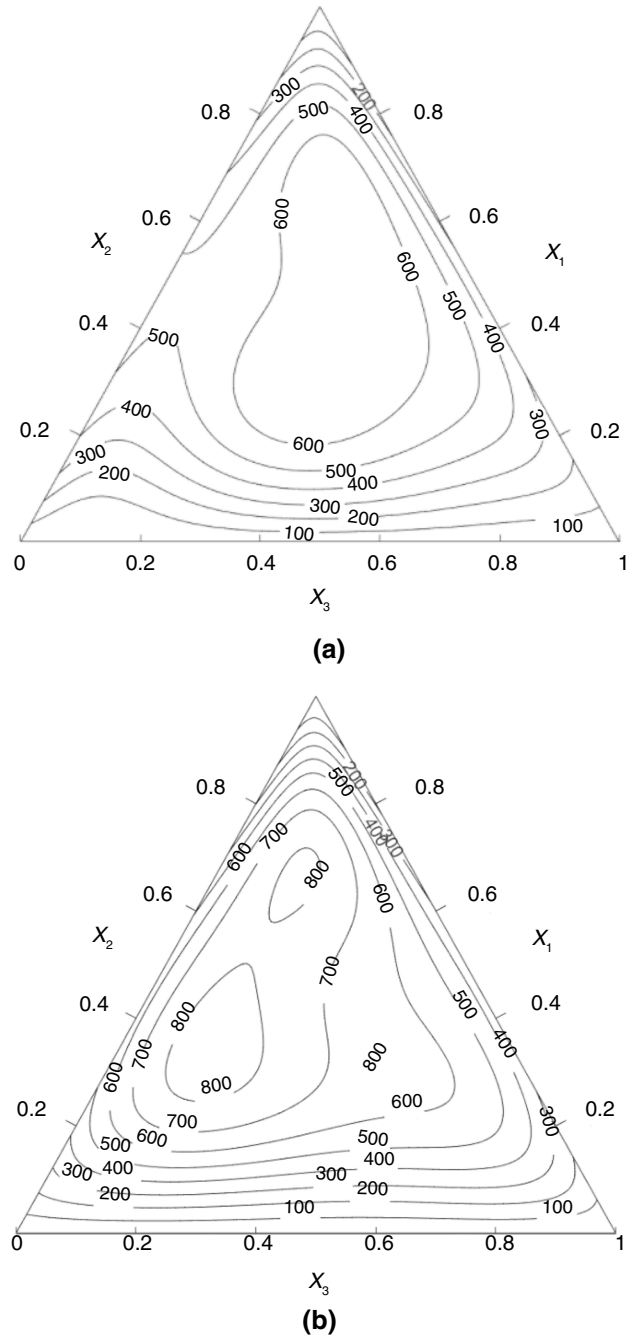

Fig. 4 Contours for constant values of H^{E}_{123} for ternary mixture diethylene glycol monoethyl ether (1) + 1-propanol (2) + ethanol (3), calculated from the representation of the experimental results by Eqs. (17 and 18) using the parameters given in Tables 5 and 6: **a**, at 298.15 K; **b**, 313.15 K. This figure is plotted using MATLAB Simulink

J·mol^{-1} at 298.15 K ($x_1 \approx 0.45$) and 557.2 J·mol^{-1} at 313.15 K ($x_1 \approx 0.45$), while the R–K correlation reproduces the experimental data with very low deviations (AAD = 0.31% at 298.15 K and 0.20% at 313.15 K). The positive excess molar enthalpies originate from the partial breakdown of strong O–H···O interactions in pure 1-PrOH and, to a lesser extent, in pure glycol ether. When mixed, these cohesive networks are replaced by weaker and more spatially dispersed cross-associations between the hydroxyl group of 1-propanol

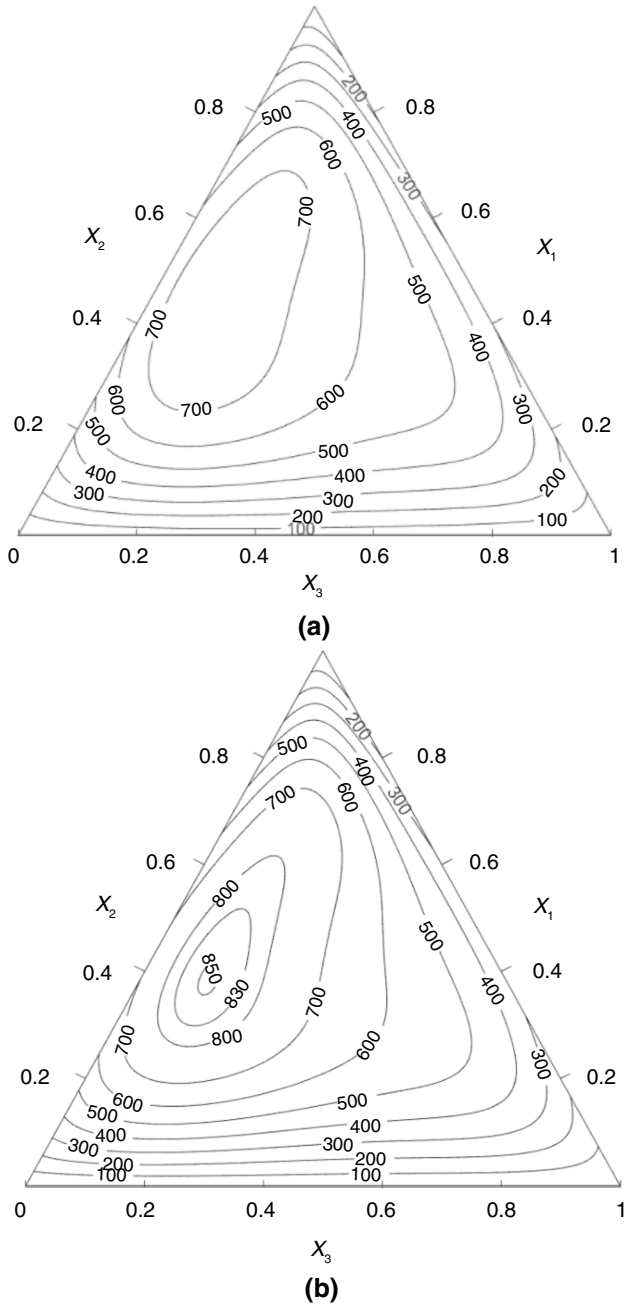

Fig. 5 Contours for constant values of H^{E}_{123} for ternary mixture ethylene glycol monomethyl ether (1) + 1-propanol (2) + ethanol (3), calculated from the representation of the experimental results by Eqs. (17 and 18) using the parameters given in Tables 5 and 6: **a**, at 298.15 K; **b**, 313.15 K. This figure is plotted using MATLAB Simulink

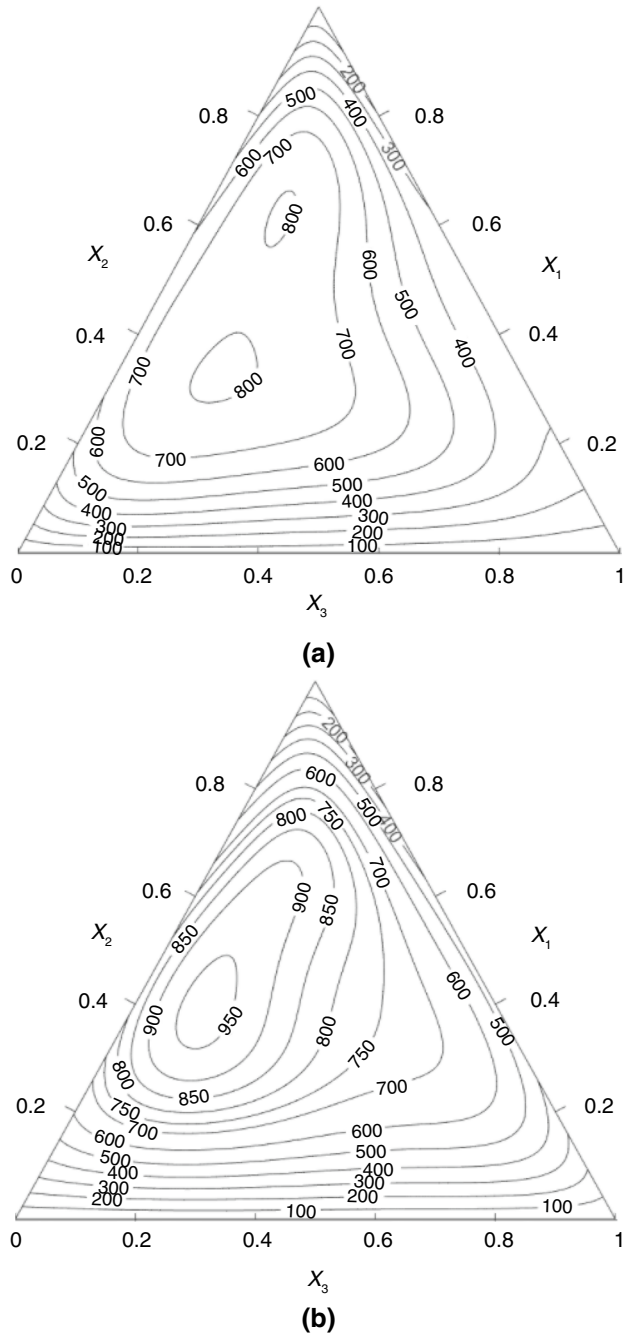

Fig. 6 Contours for constant values of H^{E}_{123} for ternary mixture ethylene glycol monophenyl ether (1) + 1-propanol (2) + ethanol (3), calculated from the representation of the experimental results by Eqs. (17 and 18) using the parameters given in Tables 5 and 6: **a**, at 298.15 K; **b**, 313.15 K. This figure is plotted using MATLAB Simulink

and the ether oxygen atoms of DEGEE, resulting in a net energetic penalty.

From a molecular viewpoint, the shape and asymmetry of the H^{E}_{m} curves can be traced to differences in structure and polarity between the two components. 1-PrOH is strongly self-associated through directional hydrogen bonds, whereas DEGEE, although bearing an OH group, has a bulky chain with multiple ether oxygens that act as hydrogen-bond acceptors but with reduced directional strength. The steric bulk of the glycol ether hinders close packing and reduces the number of strong interactions per

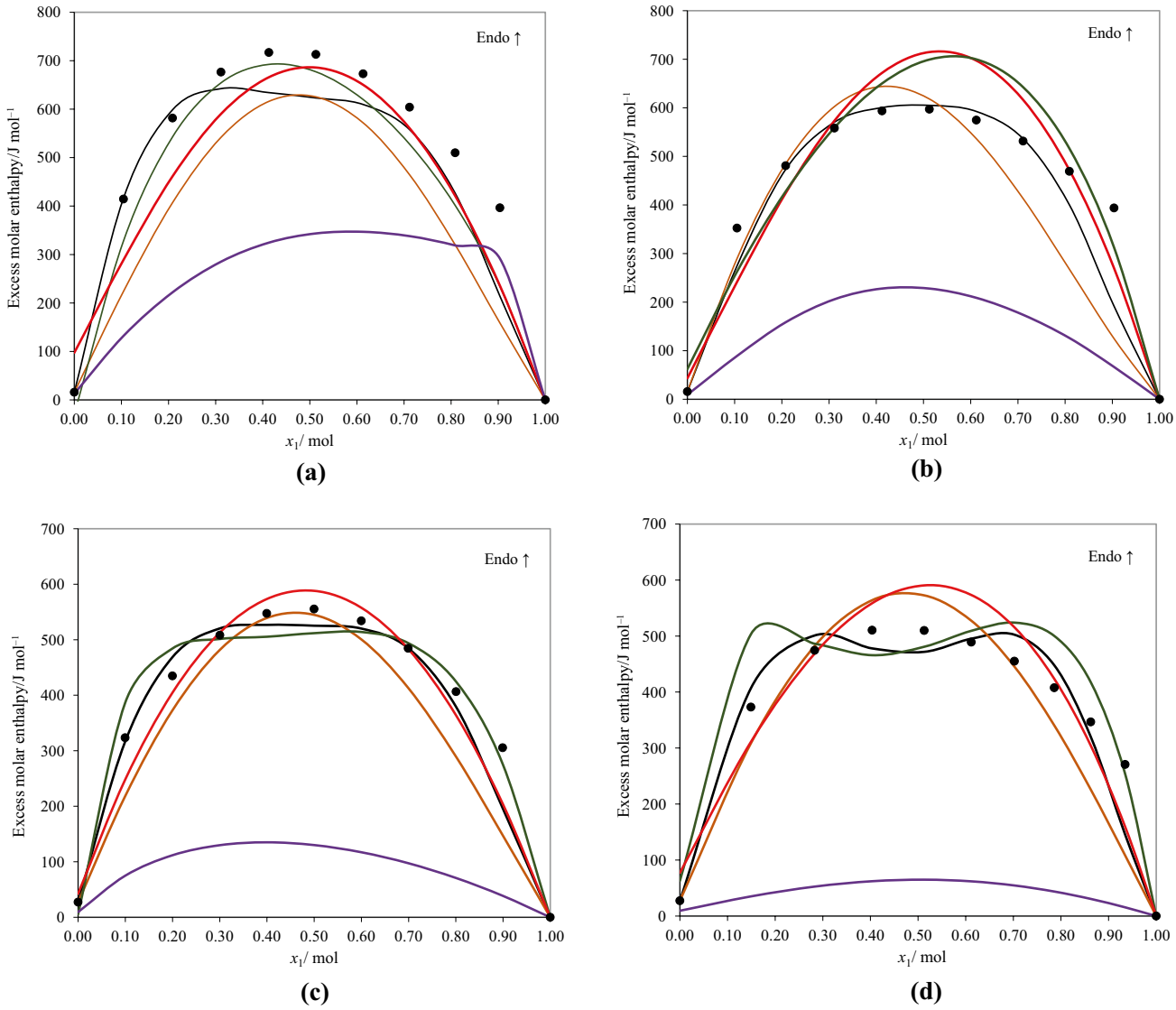

Fig. 7 Excess molar enthalpy H_m^E of ternary mixtures: **a**, diethylene glycol monomethyl ether (1) + 1-propanol (2) + ethanol (3); **b**, diethylene glycol monoethyl ether (1) + 1-propanol (2) + ethanol (3); **c**, ethylene glycol monomethyl ether (1) + 1-propanol (2) + ethanol (3); and **d**, ethylene glycol monophenyl ether (1) + 1-propanol (2) + ethanol (3). At $T = 298.15$ K and for the ratio $x_2/x_3 = 0.25$: (·), experimental data; (——), calculated values with Eq. (16); (——), calculated values with NRTL model; (——), calculated values with UNIQUAC model; (——), calculated values with UNIFAC model; and (——), calculated values with Eq. (18)

molecule. This mismatch leads to inefficient molecular organization, especially around equimolar composition, where the breaking of self-associations is most pronounced and the enthalpic deviation reaches its maximum.

With respect to model performance, the R–K equation provides the closest fit to the experimental curve, yielding the lowest deviations and accurately reproducing both the position and magnitude of the maximum. The NRTL model also offers a satisfactory representation, as its non-random mixing term effectively accounts for the heterogeneous environments created by the simultaneous presence of alcohol–alcohol, alcohol–ether, and ether–ether interactions. UNIQUAC gives a reasonable description by balancing size/shape contributions and energetic effects, though it slightly underestimates the endothermic deviations at glycol ether–rich compositions, where the steric and dipolar contributions dominate. In contrast, the modified UNIFAC (Dortmund) model captures the general convex shape but underestimates the amplitude of H_m^E, particularly at 298.15 K, due to its limited treatment of specific hydrogen bonding. Its predictions improve at 313.15 K, where hydrogen-bond contributions are weakened and dispersive plus group–group

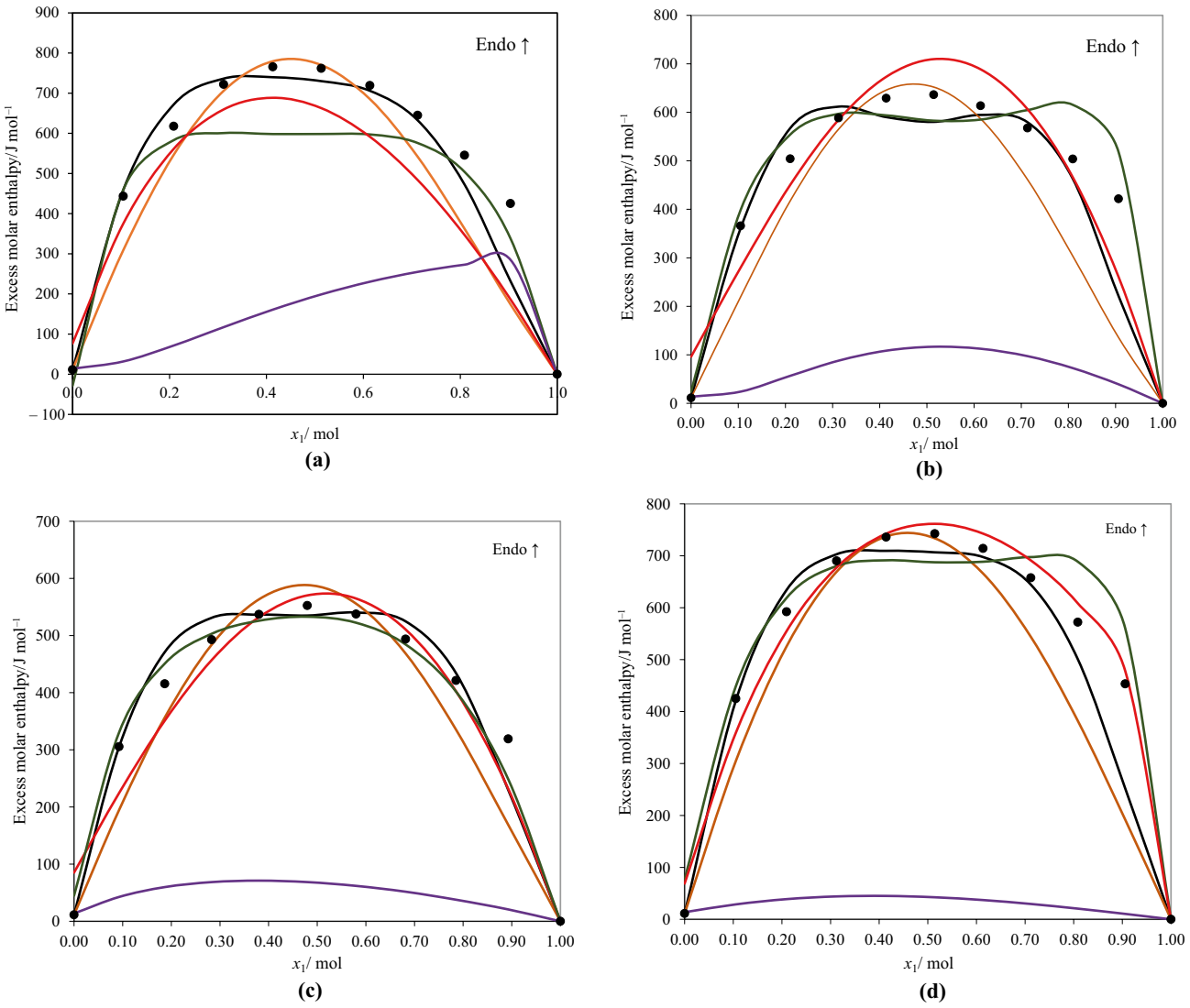

Fig. 8 Excess molar enthalpy H_m^E of ternary mixtures: **a**, diethylene glycol monomethyl ether (1) + 1-propanol (2) + ethanol (3); **b**, diethylene glycol monoethyl ether (1) + 1-propanol (2) + ethanol (3); **c**, ethylene glycol monomethyl ether (1) + 1-propanol (2) + ethanol (3); and **d**, ethylene glycol monophenyl ether (1) + 1-propanol (2) + ethanol (3). At $T = 313.15$ K and for the ratio $x_2/x_3 = 0.25$: (·), experimental data; (——), calculated values with Eq. (16); (——), calculated values with NRTL model; (——), calculated values with UNIQUAC model; (——), calculated values with UNIFAC model; and (——), calculated values with Eq. (18)

interactions play a more significant role, leading to a better match with experimental data at the higher temperature.

- EGPhE + ethanol

The H_m^E behavior of the binary mixture EGPhE + ethanol (as outlined in Fig. 4 (c)) reveals clear differences that can be attributed to molecular size, polarity, and hydrogen-bonding capabilities. The mixture reaches a maximum of 346.2 J·mol^{-1} at $x_1 = 0.3997$ and 458.5 J·mol^{-1} at $x_1 = 0.4497$ at 298.15 and 313.15 K, respectively. These results can be explained by the balance between ethanol's lower polarity and larger molecular size compared with methanol, which favors the formation of more effective hetero-interactions with EGPhE, leading to greater enthalpic deviations. On a molecular level, EGPhE possesses both an ether oxygen and an aromatic phenyl group, enabling dual interaction pathways: hydrogen bonding between the hydroxyl group of ethanol and the ether oxygen, and π–π or dipolar interactions involving the phenyl ring. The cooperative contribution of these interactions stabilizes mixed molecular arrangements, enhancing positive deviations in enthalpy [25]. In particular, the disruption of self-associated hydrogen-bonding networks of ethanol, compensated by the establishment of stronger EGPhE + ethanol-specific interactions, underlies the observed maxima in H_m^E.

Table 5 Summary of the data reduction and prediction results obtained for the studied ternary mixtures: DEGME (1) + 1-PrOH (2) + ethanol (3), DEGEE (1) + 1-PrOH (2) + ethanol (3), EGME (1) + 1-PrOH (2) + ethanol (3), and EGPhE (1) + 1-PrOH (2) + ethanol (3) at 298.15 K and at $P = 0.1$ MPa

Correlation										
DEGME (1) + 1-PrOH (2) + ethanol (3)										
ΔH^E_{123}, Eq. (17)			ΔH^E_{123}, Eq. (18)			NRTL			UNIQUAC		
B_0	J·mol^{-1}	62918.8	B_0	J·mol^{-1}	17325.6	τ_{12}	J·mol^{-1}	0.7533	Δu_{12}	J·mol^{-1}	424.6
B_1		− 136878.5	B_1		13458.5	τ_{21}		1.3184	Δu_{21}		377.8
B_2		− 307053.61	B_2		− 5540.8	τ_{13}		1.9512	Δu_{13}		181.0
B_3		81620.7	α			τ_{31}		3.1522	Δu_{31}		461.3
B_4		559563.8				τ_{23}		1.2929	Δu_{23}		− 179.4
B_5		253095				τ_{32}		− 0.5065	Δu_{32}		280.1
B_6		51146.4				α		0.39			
B_7		− 337778									
MAD (%)		15.68	MAD (%)		20.53	MAD (%)		19.94	MAD (%)		23.14
rms ΔH^E_m/J·mol^{-1}		83.4	*rms* ΔH^E_m/J·mol^{-1}		116.6	*rms* ΔH^E_m/J·mol^{-1}		99.1	*rms* ΔH^E_m/J·mol^{-1}		108.5
Max $\lvert\Delta H^E_m\rvert$/J·mol^{-1}		206.6	Max $\lvert\Delta H^E_m\rvert$/J·mol^{-1}		245.5	Max $\lvert\Delta H^E_m\rvert$/J·mol^{-1}		292.3	Max $\lvert\Delta H^E_m\rvert$/J·mol^{-1}		261.8
DEGEE (1) + 1-PrOH (2) + ethanol (3)										
ΔH^E_{123}, Eq. (17)			ΔH^E_{123}, Eq. (18)			NRTL			UNIQUAC		
B_0	J·mol^{-1}	− 12141.6	B_0	J·mol^{-1}	19446.4	τ_{12}	J·mol^{-1}	− 0.1905	Δu_{12}	J·mol^{-1}	503.3
B_1		109675.7	B_1		− 2632.3	τ_{21}		1.2064	Δu_{21}		− 26.7
B_2		60131.81	B_2		7405.07	τ_{13}		3.7763	Δu_{13}		2507.2
B_3		− 267184.3				τ_{31}	3.5569		Δu_{31}		− 814.4
B_4		− 192.39				τ_{23}	1.4248		Δu_{23}		1385.4
B_5		− 118562.17				τ_{32}	− 0.6727		Δu_{32}		− 775.0
B_6		266254.5				α	0.30				
B_7		− 83138.7									
MAD (%)		11.40	MAD (%)		16.92	MAD (%)		12.80	MAD (%)		16.13
rms ΔH^E_m/J·mol^{-1}		72.6	*rms* ΔH^E_m/J·mol^{-1}		105.4	*rms* ΔH^E_m/J·mol^{-1}		69.8	*rms* ΔH^E_m/J·mol^{-1}		99.1
Max $\lvert\Delta H^E_m\rvert$/J·mol^{-1}		200.7	Max $\lvert\Delta H^E_m\rvert$/J·mol^{-1}		281.1	Max $\lvert\Delta H^E_m\rvert$/J·mol^{-1}		148.2	Max $\lvert\Delta H^E_m\rvert$/J·mol^{-1}		239.3
EGME (1) + 1-PrOH (2) + ethanol (3)										
ΔH^E_{123}, Eq. (17)			ΔH^E_{123}, Eq. (18)			NRTL			UNIQUAC		
B_0	J·mol^{-1}	50237.2	B_0	J·mol^{-1}	18451.8	τ_{12}	J·mol^{-1}	0.5133	Δu_{12}	J·mol^{-1}	1115.0
B_1		− 118108.3	B_1		21203.1	τ_{21}		1.0233	Δu_{21}		− 280.7
B_2		− 157890.18	B_2		− 11705.9	τ_{13}		2.2235	Δu_{13}		237.3
B_3		− 45473.6				τ_{31}		3.4846	Δu_{31}		166.9
B_4		61982.3				τ_{23}		1.5075	Δu_{23}		− 563.9

Table 5 (continued)

EGME (1) + 1-PrOH (2) + ethanol (3)										
ΔH^{E}_{123}, Eq. (17)			ΔH^{E}_{123}, Eq. (18)			NRTL			UNIQUAC		
B_5		292184				τ_{32}		− 0.5077	Δu_{32}		873.5
B_6		196463.1				α		0.39			
B_7		133381									
MAD (%)		13.62	MAD (%)		21.13	MAD (%)		12.02	MAD (%)		24.72
rms ΔH^{E}_{m}/J·mol^{-1}		78.8	*rms* ΔH^{E}_{m}/J·mol^{-1}		122.0	*rms* ΔH^{E}_{m}/J·mol^{-1}		110.7	*rms* ΔH^{E}_{m}/J·mol^{-1}		120.5
Max $\lvert\Delta H^{E}_{m}\rvert$/J·mol^{-1}		242.0	Max $\lvert\Delta H^{E}_{m}\rvert$/J·mol^{-1}		355.6	Max $\lvert\Delta H^{E}_{m}\rvert$/J·mol^{-1}		308.8	Max $\lvert\Delta H^{E}_{m}\rvert$/J·mol^{-1}		365.7
EGPhE (1) + 1-PrOH (2) + ethanol (3)										
ΔH^{E}_{123}, Eq. (17)			ΔH^{E}_{123}, Eq. (18)			NRTL			UNIQUAC		
B_0	J·mol^{-1}	63597.9	B_0	J·mol^{-1}	23743.1	τ_{12}	J·mol^{-1}	0.3740	Δu_{12}	J·mol^{-1}	529.1
B_1		− 120927.1	B_1		25901.5	τ_{21}		1.2413	Δu_{21}		164.0
B_2		− 232854.96	B_2		− 11192.7	τ_{13}		2.8490	Δu_{13}		1877.0
B_3		− 116554.9				τ_{31}		4.6988	Δu_{31}		− 712.5
B_4		194413.5				τ_{23}		1.8536	Δu_{23}		1758.3
B_5		361708				τ_{32}		− 0.6707	Δu_{32}		− 908.9
B_6		286183.6				α		0.20			
B_7		58468									
MAD (%)		14.27	MAD (%)		22.11	MAD (%)		14.25	MAD (%)		26.23
rms ΔH^{E}_{m}/J·mol^{-1}		106.3	*rms* ΔH^{E}_{m}/J·mol^{-1}		158.1	*rms* ΔH^{E}_{m}/J·mol^{-1}		143.0	*rms* ΔH^{E}_{m}/J·mol^{-1}		159.9
Max $\lvert\Delta H^{E}_{m}\rvert$/J·mol^{-1}		356.1	Max $\lvert\Delta H^{E}_{m}\rvert$/J·mol^{-1}		502.1	Max $\lvert\Delta H^{E}_{m}\rvert$/J·mol^{-1}		478.4	Max $\lvert\Delta H^{E}_{m}\rvert$/J·mol^{-1}		555.0
Prediction										
DEGME (1) + 1-PrOH (2) + ethanol (3)										
NRTL						UNIQUAC				
τ_{12}		J·mol^{-1}	0.6746			Δu_{12}		J·mol^{-1}	429.70		
τ_{21}			0.3422			Δu_{21}			169.33		
τ_{13}			1.2413			Δu_{13}			595.9		
τ_{31}			0.0247			Δu_{31}			482.42		
τ_{23}			0.9587			Δu_{23}			28.39		
τ_{32}			0.2066			Δu_{32}			453.10		
α_{12}			0.20								
α_{13}			0.20								
α_{23}			0.20								
MAD (%)			24.88			MAD (%)			22.26		
rms ΔH^{E}_{m}/J·mol^{-1}			158.3			*rms* ΔH^{E}_{m}/J·mol^{-1}			112.8		
Max $\lvert\Delta H^{E}_{m}\rvert$/J·mol^{-1}			245.8			Max $\lvert\Delta H^{E}_{m}\rvert$/J·mol^{-1}			189.3		

Table 5 (continued)

DEGEE (1) + 1-PrOH (2) + ethanol (3)					
NRTL			UNIQUAC		
τ_{12}	J·mol^{-1}	0.1119	Δu_{12}	J·mol^{-1}	429.74
τ_{21}		1.0566	Δu_{21}		283.06
τ_{13}		− 0.0879	Δu_{13}		758.74
τ_{31}		0.7691	Δu_{31}		− 301.87
τ_{23}		0.2063	Δu_{23}		748.65
τ_{32}		− 0.1502	Δu_{32}		− 522.17
α_{12}		0.20			
α_{13}		0.20			
α_{23}		0.20			
MAD (%)		28.72	MAD (%)		29.48
rms ΔH_m^E/J·mol^{-1}		135.4	*rms* ΔH_m^E/J·mol^{-1}		136.5
Max $\lvert\Delta H_m^E\rvert$/J·mol^{-1}		258.8	Max $\lvert\Delta H_m^E\rvert$/J·mol^{-1}		263.3
EGME (1) + 1-PrOH (2) + ethanol (3)					
NRTL			UNIQUAC		
τ_{12}	J·mol^{-1}	0.3620	Δu_{12}	J·mol^{-1}	716.80
τ_{21}		0.7013	Δu_{21}		− 124.8
τ_{13}		0.1010	Δu_{13}		836.44
τ_{31}		0.4613	Δu_{31}		− 368.11
τ_{23}		0.2066	Δu_{23}		453.55
τ_{32}		− 0.1504	Δu_{32}		− 359.76
α_{12}		0.20			
α_{13}		0.20			
α_{23}		0.20			
MAD (%)		32.4	MAD (%)		19.3
rms $\Delta \boldsymbol{H}_m^E$/J·mol^{-1}		199.9	*rms* ΔH_m^E/J·mol^{-1}		215.4
Max $\lvert\Delta \boldsymbol{H}_m^E\rvert$/J·mol^{-1}		416.1	Max $\lvert\Delta H_m^E\rvert$/J·mol^{-1}		448.2
EGPhE (1) + 1-PrOH (2) + ethanol (3)					
NRTL			UNIQUAC		
τ_{12}	J·mol^{-1}	0.3424	Δu_{12}	J·mol^{-1}	606.93
τ_{21}		0.7969	Δu_{21}		− 20.3
τ_{13}		− 0.0687	Δu_{13}		384.29
τ_{31}		0.8504	Δu_{31}		15.79
τ_{23}		− 0.0081	Δu_{23}		− 40.47

Table 5 (continued)

EGPhE (1) + 1-PrOH (2) + ethanol (3)			
NRTL		UNIQUAC	
τ_{32}	0.0455	Δu_{32}	72.44
α_{12}	0.20		
α_{13}	0.20		
α_{23}	0.20		
MAD (%)	40.26	MAD (%)	42.71
rms ΔH_m^E/J·mol^{-1}	274.2	*rms* ΔH_m^E/J·mol^{-1}	300.7
Max $\lvert\Delta H_m^E\rvert$/J·mol^{-1}	602.9	Max $\lvert\Delta H_m^E\rvert$/J·mol^{-1}	638.1

DEGME Diethylene glycol monomethyl ether, *DEGEE* Diethylene glycol monoethyl ether, *EGME* Ethylene glycol monomethyl ether, and *EGPhE* Ethylene

Among the thermodynamic models applied, the R–K equation consistently provides the best fit for the ethanol system, with rms ΔH_m^E of 5.55 J·mol^{-1} at 298.15 K. The UNIQUAC and NRTL models also show fair agreement but with slightly higher deviations, 11.80 J·mol^{-1} and 12.92 J·mol^{-1}, respectively. In contrast, the modified UNIFAC (Dortmund) model tends to overestimate the excess molar enthalpy, reflecting its limited ability to explicitly capture directional and specific hydrogen-bonding interactions.

The ternary systems [DEGME (1) + 1-PrOH (2) + ethanol (3)], [DEGEE (1) + 1-BuOH (2) + ethanol (3)], [EGME (1) + 1-PrOH (2) + ethanol (3)], and [EGPhE (1) + 1-PrOH (2) + ethanol (3)] were obtained by introducing glycol ethers into the binary systems 1-BuOH + ethanol, and their excess molar enthalpies were determined at 298.15 K and 313.15 K. For each ternary system, four different initial binary compositions were selected, with x_2/x_3 ratios fixed at 0.2500, 0.6667, 1.5000, and 4.0000, respectively.

The experimental results of H_m^E at 298.15 and 313.15 are reported in Tables S1 and S2, respectively. These values were determined using Eq. (15):

$$H_{123}^E = H_{1+23}^E + \left(1 - x_2\right)H_{23}^E \tag{15}$$

where H_{1+23}^E represents the experimental values of the ternary blends, and H_{23}^E corresponds to the R–K equation of the binary ethanol + 1-propanol blend. The temperature and composition dependence of the ternary blends is shown in Figs. 3–6.

The experimental data were further fitted using Eq. (16):

$$H_{123}^E = H_{12}^E + H_{13}^E + H_{23}^E + x_1x_2x_3\Delta H_{123}^E \tag{16}$$

with

$$\Delta H_{123}^E = B_0 + B_1x_1 + B_2x_2 + B_3x_1^2 + B_4x_2^2 + B_5x_1x_2 + B_6x_1^3 + B_7x_2^3 \tag{17}$$

The B_i parameters were determined using the unweighted least-squares method. Additionally, ΔH_{123}^E can be also calculated with:

$$\Delta H_{123}^E = B_1x_1 + B_2x_2 + B_3x_3 \tag{18}$$

Tables 5 and 6 provide an overview of the reduction and prediction results outcomes for the ternary mixtures, based on the parameters derived from the corresponding binary systems.

- DEGME + 1-PrOH + ethanol

Endothermic behavior was observed, as indicated by the positive excess molar enthalpy H_m^E values across the entire range of composition at the studied temperatures (Fig. 3). The maximum experimental H_m^E for this blend is

Table 6 Summary of the data reduction and prediction results obtained for the studied ternary mixtures: DEGME (1) + 1-PrOH (2) + ethanol (3), DEGEE (1) + 1-PrOH (2) + ethanol (3), EGME (1) + 1-PrOH (2) + ethanol (3), and EGPhE (1) + 1-PrOH (2) + ethanol (3) at 313.15 K and at $P = 0.1$ MPa

Correlation										
DEGME (1) + 1-PrOH (2) + ethanol (3)										
ΔH^E_{123}, Eq. (17)			ΔH^E_{123}, Eq. (18)			NRTL			UNIQUAC		
B_0	J·mol^{-1}	38072.4	B_0	J·mol^{-1}	24765.1	τ_{12}	J·mol^{-1}	0.4248	Δu_{12}	J·mol^{-1}	694.9
B_1		− 52472.1	B_1		8536.6	τ_{21}		1.4206	Δu_{21}		198.4
B_2		− 125536.99	B_2		2319.7	τ_{13}		2.4892	Δu_{13}		159.6
B_3		− 73347.8	α			τ_{31}		4.7725	Δu_{31}		577.7
B_4		165974.7				τ_{23}		1.5173	Δu_{23}		− 427.2
B_5		131546				τ_{32}		− 0.6732	Δu_{32}		658.0
B_6		182835.5				α		0.29			
B_7		− 56575									
MAD (%)		8.39	MAD (%)		16.06	MAD (%)		12.17	MAD (%)		19.42
rms ΔH^E_m/J·mol^{-1}		44.8	*rms* ΔH^E_m/J·mol^{-1}		93.7	*rms* ΔH^E_m/J·mol^{-1}		115.4	*rms* ΔH^E_m/J·mol^{-1}		114.2
Max $\lvert\Delta H^E_m\rvert$/J·mol^{-1}		143.3	Max $\lvert\Delta H^E_m\rvert$/J·mol^{-1}		248.2	Max $\lvert\Delta H^E_m\rvert$/J·mol^{-1}		378.2	Max $\lvert\Delta H^E_m\rvert$/J·mol^{-1}		215.8
DEGEE (1) + 1-PrOH (2) + ethanol (3)										
ΔH^E_{123}, Eq. (17)			ΔH^E_{123}, Eq. (18)			NRTL			UNIQUAC		
B_0	J·mol^{-1}	29597.3	B_0	J·mol^{-1}	28854.82	τ_{12}	J·mol^{-1}	1.0786	Δu_{12}	J·mol^{-1}	914.42
B_1		33066.0	B_1		7916.1	τ_{21}		1.4570	Δu_{21}		32.08
B_2		− 136277.15	B_2		− 1143.27	τ_{13}		4.2799	Δu_{13}		2122.12
B_3		− 321940.6				τ_{31}		2.4766	Δu_{31}		− 662.10
B_4		201176.41				τ_{23}		− 0.3046	Δu_{23}		− 519.61
B_5		135260.11				τ_{32}		0.4332	Δu_{32}		855.74
B_6		401461.7				α		0.30			
B_7		− 84567.4									
MAD (%)		10.28	MAD (%)		19.33	MAD (%)		5.41	MAD (%)		10.54
rms ΔH^E_m/J·mol^{-1}		83.7	*rms* ΔH^E_m/J·mol^{-1}		136.8	*rms* ΔH^E_m/J·mol^{-1}		42.3	*rms* ΔH^E_m/J·mol^{-1}		79.9
Max $\lvert\Delta H^E_m\rvert$/J·mol^{-1}		242.1	Max $\lvert\Delta H^E_m\rvert$/J·mol^{-1}		319.8	Max $\lvert\Delta H^E_m\rvert$/J·mol^{-1}		115.6	Max $\lvert\Delta H^E_m\rvert$/J·mol^{-1}		188.2
EGME (1) + 1-PrOH (2) + ethanol (3)										
ΔH^E_{123}, Eq. (17)			ΔH^E_{123}, Eq. (18)			NRTL			UNIQUAC		
B_0	J·mol^{-1}	26185.1	B_0	J·mol^{-1}	16944.8	τ_{12}	J·mol^{-1}	1.2311	Δu_{12}	J·mol^{-1}	1177.7
B_1		− 24017.7	B_1		8183.2	τ_{21}		0.3242	Δu_{21}		− 158.1
B_2		− 87580.06	B_2		414.4	τ_{13}		1.4601	Δu_{13}		1685.6
B_3		− 118906.8				τ_{31}		4.6803	Δu_{31}		− 624.8
B_4		110652.79				τ_{23}		102.698	Δu_{23}		− 577.4

Table 6 (continued)

EGME (1) + 1-PrOH (2) + ethanol (3)									
ΔH^{E}_{123}, Eq. (17)			ΔH^{E}_{123}, Eq. (18)			NRTL			UNIQUAC		
B_5		104174.27				τ_{32}		0.1090	Δu_{32}		930.5
B_6		199830.4				α		0.30			
B_7		− 30581.4									
MAD (%)		9.7	MAD (%)		14.9	MAD (%)		6.6	MAD (%)		8.8
rms ΔH^{E}_{m}/J·mol^{-1}		69.6	*rms* ΔH^{E}_{m}/J·mol^{-1}		89.6	*rms* ΔH^{E}_{m}/J·mol^{-1}		43.2	*rms* ΔH^{E}_{m}/J·mol^{-1}		56.6
Max $\lvert\Delta H^{E}_{m}\rvert$/J·mol^{-1}		132.8	Max $\lvert\Delta H^{E}_{m}\rvert$/J·mol^{-1}		172.8	Max $\lvert\Delta H^{E}_{m}\rvert$/J·mol^{-1}		99.6	Max $\lvert\Delta H^{E}_{m}\rvert$/J·mol^{-1}		122.8
EGPhE (1) + 1-PrOH (2) + ethanol (3)											
ΔH^{E}_{123}, Eq. (17)			ΔH^{E}_{123}, Eq. (18)			NRTL			UNIQUAC		
B_0	J·mol^{-1}	31245.0	B_0	J·mol^{-1}	19256.9	τ_{12}	J·mol^{-1}	1.9402	Δu_{12}	J·mol^{-1}	45.59
B_1		− 14504.1	B_1		6487.4	τ_{21}		2.2103	Δu_{21}		1220.42
B_2		− 125597.2	B_2		2800.3	τ_{13}		4.2010	Δu_{13}		8465.71
B_3		− 147070.3				τ_{31}		2.0423	Δu_{31}		905.05
B_4		208619.2				τ_{23}		− 0.5747	Δu_{23}		225.64
B_5		97242.40				τ_{32}		1.0956	Δu_{32}		− 45.69
B_6		226198.4				α		0.30			
B_7		− 108389.2									
MAD (%)		7.5	MAD (%)		14.6	MAD (%)		4.2	MAD (%)		6.0
rms ΔH^{E}_{m}/J·mol^{-1}		48.3	*rms* ΔH^{E}_{m}/J·mol^{-1}		85.3	*rms* ΔH^{E}_{m}/J·mol^{-1}		33.2	*rms* ΔH^{E}_{m}/J·mol^{-1}		54.8
Max $\lvert\Delta H^{E}_{m}\rvert$/J·mol^{-1}		174.7	Max $\lvert\Delta H^{E}_{m}\rvert$/J·mol^{-1}		213.7	Max $\lvert\Delta H^{E}_{m}\rvert$/J·mol^{-1}		116.5	Max $\lvert\Delta H^{E}_{m}\rvert$/J·mol^{-1}		160.7
Prediction											
DEGME (1) + 1-PrOH (2) + ethanol (3)											
NRTL						UNIQUAC					
τ_{12}		J·mol^{-1}	0.3146			Δu_{12}		J·mol^{-1}	− 71.23		
τ_{21}			1.2572			Δu_{21}			862.0		
τ_{13}			0.0292			Δu_{13}			320.82		
τ_{31}			0.9489			Δu_{31}			239.82		
τ_{23}			0.2242			Δu_{23}			− 82.41		
τ_{32}			− 0.1705			Δu_{32}			109.97		
α_{12}			0.20								
α_{13}			0.20								
α_{23}			0.20								
MAD (%)			33.06			MAD (%)			38.90		
rms ΔH^{E}_{m}/J·mol^{-1}			191.3			*rms* ΔH^{E}_{m}/J·mol^{-1}			239.7		

Table 6 (continued)

Prediction					
DEGME (1) + 1-PrOH (2) + ethanol (3)					
NRTL			UNIQUAC		
Max $\lvert\Delta H_m^E\rvert$/J·mol^{-1}		262.2	Max $\lvert\Delta H_m^E\rvert$/J·mol^{-1}		344.8
DEGEE (1) + 1-PrOH (2) + ethanol (3)					
NRTL			UNIQUAC		
τ_{12}	J·mol^{-1}	0.1268	Δu_{12}	J·mol^{-1}	56.59
τ_{21}		1.0564	Δu_{21}		417.61
τ_{13}		− 0.0724	Δu_{13}		826.15
τ_{31}		0.7675	Δu_{31}		− 327.15
τ_{23}		0.2227	Δu_{23}		518.06
τ_{32}		− 0.1693	Δu_{32}		− 410.81
α_{12}		0.20			
α_{13}		0.20			
α_{23}		0.20			
MAD (%)		41.17	MAD (%)		43.61
rms ΔH_m^E/J·mol^{-1}		199.9	*rms* ΔH_m^E/J·mol^{-1}		231.1
Max $\lvert\Delta H_m^E\rvert$/J·mol^{-1}		301.3	Max $\lvert\Delta H_m^E\rvert$/J·mol^{-1}		374.9
EGME (1) + 1-PrOH (2) + ethanol (3)					
NRTL			UNIQUAC		
τ_{12}	J·mol^{-1}	0.3910	Δu_{12}	J·mol^{-1}	214.03
τ_{21}		1.1097	Δu_{21}		448.03
τ_{13}		0.0907	Δu_{13}		1033.05
τ_{31}		0.4903	Δu_{31}		− 450.24
τ_{23}		0.2227	Δu_{23}		474.98
τ_{32}		− 0.1693	Δu_{32}		− 377.67
α_{12}		0.20			
α_{13}		0.20			
α_{23}		0.20			
MAD (%)		25.7	MAD (%)		26.2
rms $\Delta \boldsymbol{H}_m^E$/J·mol^{-1}		92.5	*rms* ΔH_m^E/J·mol^{-1}		100.4
Max $\lvert\Delta \boldsymbol{H}_m^E\rvert$/J·mol^{-1}		144.3	Max $\lvert\Delta H_m^E\rvert$/J·mol^{-1}		181.0

Table 6 (continued)

EGPhE (1) + 1-PrOH (2) + ethanol (3)					
NRTL			UNIQUAC		
τ_{12}	J·mol^{-1}	0.6016	Δu_{12}	J·mol^{-1}	7.88
τ_{21}		1.1842	Δu_{21}		1014.25
τ_{13}		0.0787	Δu_{13}		385.57
τ_{31}		0.8380	Δu_{31}		287.49
τ_{23}		0.2227	Δu_{23}		474.98
τ_{32}		− 0.1693	Δu_{32}		− 377.67
α_{12}		0.20			
α_{13}		0.20			
α_{23}		0.20			
MAD (%)		28.3	MAD (%)		19.2
rms ΔH_m^E/J·mol^{-1}		138.3	*rms* ΔH_m^E/J·mol^{-1}		95.5
Max $\lvert\Delta H_m^E\rvert$/J·mol^{-1}		242.6	Max $\lvert\Delta H_m^E\rvert$/J·mol^{-1}		258.4

DEGME Diethylene glycol monomethyl ether, *DEGEE* Diethylene glycol monoethyl ether, *EGME* Ethylene glycol monomethyl ether, *EGPhE* Ethylene glycol monophenyl ether, and *1-PrOH* 1-propanol

Table 7 Modified UNIFAC (Dortmund) group interaction parameters used in this work [22]

Main group		Group interaction parameters		
1	2	a_{12}/K a_{21}/K	b_{12}/K b_{21}/K	c_{12}/K^{-1} c_{21}/K^{-1}
CH_2	OH	2777 1606	− 4.674 − 4.746	0.001551 0.0009181
CH_2	CH_2O	233.1 − 9.654	− 0.3155 − 0.03242	N/A N/A
CH_2	ACOH	1381 1987	− 0.9977 − 4.615	N/A N/A
OH	CH_2O	816.7 650.9	− 5.092 − 0.7132	0.00606 0.000815
OH	ACOH	83.91 465.4	− 1.262 − 1.841	N/A N/A

945.4 J·mol^{-1} at 298.15 K and 1169.4 J·mol^{-1} at 315.15 K corresponding to $x_1 = 0.4438$, $x_2 = 0.4466$, and $x_3 = 0.1095$. The lowest AAD (15.68%) at $T = 298.15$ K was achieved with ΔH^E_{123}, Eq. (17), comparably to ΔH^E_{123}, Eq. (18), UNIQUAC, NRTL, and modified UNIFAC models (20.53%, 23.14%, 19.94%, and 52.81%). At $T = 313.15$ K, the best AAD and rms (8.39%, 44.8 J·mol^{-1}) are achieved with ΔH^E_{123}, Eq. (17). Generally, ΔH^E_{123}, Eq. (18), and NRTL demonstrated comparable accuracy, both outperforming the UNIQUAC and UNIFAC models.

DEGME contains one hydroxyl group and one ether oxygen, giving it both hydrogen-bond donor and acceptor sites. This dual functionality allows DEGME molecules to engage in self-association through O–H···O hydrogen bonding. In the ternary mixture with ethanol and 1-PrOH, the strong alcohol–alcohol hydrogen-bond network is partially disrupted, while the new cross-interactions involving DEGME are weaker and cannot fully compensate for the loss of self-association. This imbalance results in positive excess molar enthalpies. Furthermore, the longer alkyl chain of 1-PrOH enhances hydrophobic segregation effects when combined with DEGME and ethanol, thereby increasing the enthalpic penalty upon mixing. The UNIFAC (Dortmund) model shows poor predictive performance for this system, reflecting its limitations in capturing the competition between multiple hydrogen-bonding sites and the steric/hydrophobic mismatch among the three components.

- DEGEE + 1-PrOH + ethanol

A similar endothermic behavior was observed for the mixture DEGME + 1-PrOH + ethanol, supported by positive H^E_m values at the two investigated temperatures, as shown in Fig. 4. The maximum excess molar enthalpy H^E_m for this blend is 724.2 J·mol^{-1} at 298.15 K and 861.6 J·mol^{-1} at

Table 8 Molecular formulae of the species in this work, shown as structures of subgroups for group-contribution models

Component*	Structure	Molecular formula
DEGME	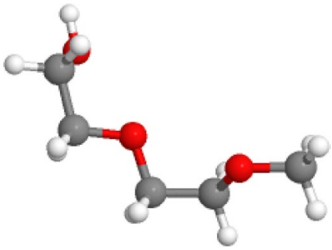	$CH_3O–CH_2–CH_2O–CH_2–CH_2–OH$
DEGEE	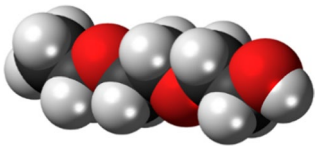	$CH_3–CH_2O–CH_2–CH_2O–CH_2–CH_2–OH$
EGME	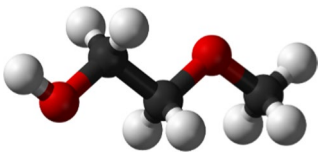	$CH_3O–CH_2–CH_2–OH$
EGPhE	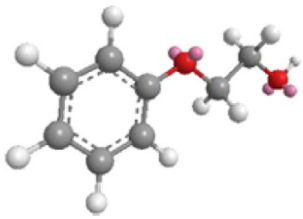	$C_6H_5O–CH_2–CH_2–OH$
Ethanol		$CH_3–CH_2–OH$
1-Propanol	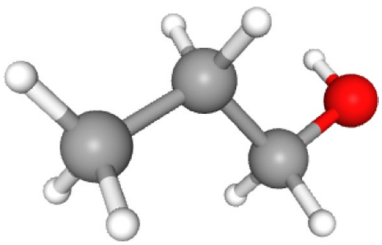	$CH_3–CH_2–CH_2–OH$

**DEGME* Diethylene glycol monomethyl ether, *DEGEE* Diethylene glycol monoethyl ether, *EGME* Ethylene glycol monomethyl ether, *EGPhE* Ethylene glycol monophenyl ether, and *1-PrOH* 1-propanol

313.15 K corresponding to $x_1 = 0.4332$, $x_2 = 0.3347$, and $x_3 = 0.2320$. At 298.15 K, ΔH^E_{123}, Eq. (17), gives the best representation of the experimental data, with the lowest deviations in terms of AAD (11.4%). However, the NRTL model yields superior agreement when evaluated by rms (69.8 J·mol^{-1}) and maximum deviation (Max $|\Delta H^E_m| = 148.2$ J·mol^{-1}), showing that it better captures the magnitude of enthalpic fluctuations. A similar trend is observed at 313.15 K, where NRTL again provides the smallest errors (AAD = 5.41%, rms = 42.3 J·mol^{-1}, Max $|\Delta H^E_m| = 115.6$ J·mol^{-1}). These results confirm that the NRTL model is the most reliable among those tested for describing the thermodynamic behavior of the system at both temperatures.

Structurally, DEGME differs from DEGEE by having a methyl rather than an ethyl substituent. This substitution makes DEGME less hydrophobic and slightly more polar. The higher polarity of DEGME enhances its tendency for

Table 9 Modified UNIFAC (Dortmund) relative van der Waals volumes R_K and surface areas Q_K [22]

Main group	Subgroup	R_K	Q_K
CH_2	CH_3	0.6325	1.0608
	CH_2	0.6325	0.7081
OH	OH	1.2302	0.8927
CH_2O	CH_3O	1.1434	1.6022
	CH_2O	1.1434	1.2495
	CHO	1.1434	0.8968
ACOH	ACOH	1.080	0.9750

self-association compared to DEGEE, although still weaker than that of DEGEE. Consequently, the magnitude of H^E_m is somewhat reduced. Nevertheless, mixing with ethanol and 1-PrOH still involves the disruption of strong alcohol–alcohol hydrogen-bond networks, while the newly formed cross-associations are energetically less favorable, leading overall to positive excess molar enthalpies. The UNIFAC (Dortmund) model performs poorly for this system, showing that group-contribution methods do not capture the subtle differences in chain length and polarity that strongly influence association equilibria.

- EGME + 1-PrOH + ethanol

The EGME + 1-PrOH + ethanol blend also showed endothermic behavior with positive H^E_m values over the entire composition range at both temperatures considered (Fig. 5). The maximum excess molar enthalpy H^E_m is 944.3 J·mol^{-1} at 298.15 K and 773.9 J·mol^{-1}, at 313.15 K related to $x_1 = 0.5235$, $x_2 = 0.3768$, and $x_3 = 0.0982$. At 298.15 K, the NRTL model provides the lowest average absolute deviation (AAD = 12.02%), indicating the best fit in terms of relative error. In contrast, Eq. (17) achieves the lowest rms (78.8 J·mol^{-1}) and the smallest maximum deviation (Max $|\Delta H^E_m| = 242.0$ J·mol^{-}1), outperforming Eq. (18) and UNIQUAC in capturing the magnitude of enthalpic variations. At T = 313.15 K, UNIQUAC model and ΔH^E_{123}, Eq. (17), are the best with AAD (6.6%, 8.8%), *rms* (43.2 J·mol^{-1}, 56.6 J·mol^{-1}), and Max $|\Delta H^E_m|$ (99.6 J·mol^{-1}, 122.8 J·mol^{-1}). These models demonstrated better accuracy than UNIQUAC and UNIFAC models.

EGME is smaller than the diethylene glycol monoethers (DEGME, DEGEE) and has only one ether oxygen, yet it still forms strong hydrogen-bonded structures [26]. On mixing, disruption of ethanol–ethanol and ethanol–butanol associations leads to a positive enthalpy, but the magnitude is lower than for DEGME because the steric hindrance is less pronounced and cross-interactions with ethanol are more favorable. The modified UNIFAC approach again shows significant errors, which highlights its limitation in representing size-dependent and polarity-driven interactions.

- EGPhE + 1-PrOH + ethanol

For the EGPhE + 1-PrOH + ethanol blend, endothermic behavior was confirmed by positive H^E_m for all mole fractions at both investigated temperatures (Fig. 6). The maximum excess molar enthalpy H^E_m was 1076.7 J·mol^{-1} at 298.15 K corresponding to $x_1 = 0.5437$, $x_2 = 0.3617$, and $x_3 = 0.0946$ and increased to 988.8 J·mol^{-1} at 315.15 K corresponding to $x_1 = 0.4408$, $x_2 = 0.4432$, and $x_3 = 0.1160$. At 298.15 K, ΔH^E_{123}, Eq. (17), has the lowest ADD, rms, and Max $|\Delta H^E_m|$ (14.2%, 106.3 J·mol^{-1}, and 356.1 J·mol^{-1}). At $T = 313.15$ K, the minimum AAD (4.2%), rms (33.2 J·mol^{-1}), and Max $|\Delta H^E_m|$ (116.5 J·mol^{-1}) are found for NRTL model.

The strong endothermicity of this system originates from the molecular features of EGPhE. The aromatic ring introduces π–π interactions and increases the hydrophobicity of the molecule, making it less compatible with ethanol and 1-PrOH [27]. When the mixture forms, both the aromatic self-association of EGPhE and the hydrogen-bonded alcohol structures are disrupted, but the cross-interactions are not strong enough to compensate. This results in the highest positive H^E_m values among the systems studied. The UNIFAC (Dortmund) model fails drastically, mainly because the group parameters do not explicitly account for aromatic-specific interactions or the anisotropy of phenoxy substitution.

For the ternary blends of DEGME + 1-PROH + ethanol and DEGEE + 1-PrOH + ethanol at 298.15 K, the ΔH^E_{123}, Eq. (17), provides the best agreement with experimental data compared to ΔH^E_{123}, Eq. (18), NRTL, UNIQUAC, and UNIFAC. At 313.15 K, ΔH^E_{123}, Eq. (17), again gives the lowest deviations for the system containing DEGME, with AAD = 8.39%, rms = 44.8 J·mol^{-}1, and Max $|\Delta H^E_m| = 143.3$ J·mol^{-1}. For the mixture with DEGEE at the same temperature, the deviations obtained with NRTL are AAD = 5.41%, rms = 42.3 J·mol^{-1}, and Max $|\Delta H^E_m| = 115.6$ J·mol^{-1}. However, for this blend at 313.15 K, ΔH^E_{123}, Eq. (17), outperforms the other models, yielding the lowest deviations (AAD = 10.28%, rms = 83.7 J·mol^{-1}, and Max $|\Delta H^E_m| = 242.1$ J·mol^{-1}). NRTL also shows the best performance at 298.15 K for the EGME + 1-PrOH + ethanol system (AAD = 12.02%, rms = 110.7 J·mol^{-1}, and Max |Δ

H_m^E|= 308.8 J·mol^{-1}) and for the EGPhE + 1-PrOH + ethanol system (AAD = 14.2%), although in the latter case, ΔH_{123}^E, Eq. (17), gives the lowest rms and Max |ΔH_m^E| (106.3 J·mol^{-1} and 275.5 J·mol^{-1}). At 313.15 K, the NRTL model performs better for the EGME + 1-PrOH + ethanol mixture, with the lowest AAD, rms, and Max |ΔH_m^E| (6.6% 43.2 J·mol^{-1}and 99.6 J·mol^{-1}). For the EGPhE + 1-PrOH + ethanol blend at this temperature, the NRTL model provides the most accurate prediction, with the smallest deviations (AAD = 4.2%, rms = 33.2 J·mol^{-1}, Max |ΔH_m^E|= 116.5 J·mol^{-1}).

Table 8 presents the molecular formulae of the species studied, illustrated as subgroups structures used in group-contribution models. The studied liquids differ in molecular size, shape, and interaction potential. Across all ternary mixtures, positive H_m^E *v*alues confirmed endothermic behavior, attributed to weak intermolecular interactions. At constant pressure, excess molar enthalpy increased as temperature rose from 298.15 to 323.15 K in all mixtures: DEGME + 1-PrOH + ethanol, DEGEE + 1- PrOH + ethanol, EGME + 1- PrOH + ethanol, EGPhE + 1- PrOH + ethanol. This increase is likely due to the relatively low polarity and weak associative interactions among the molecules. As temperature increases, hydrogen bonds (alcohol–alcohol and alcohol–ether) weaken, leading to an increase in H_m^E. Glycol ethers improve miscibility between highly polar ethanol and less polar butanol. However, at higher temperatures, the effect of glycol ethers is reduced, weakening dipolar interactions and contributing to increased excess molar enthalpy.

Conclusions

In order to assess their relevance for fuel applications, particular attention was given to the molecular interactions and structural features of oxygenated additives. The excess molar enthalpies (H_m^E) of the binary system composed of ethanol and 1-PrOH were determined at 298.15 K and 313.15 K under atmospheric pressure (0.1 MPa). Ternary mixtures were subsequently prepared by introducing different glycol ethers: diethylene glycol monomethyl ether (DEGME), diethylene glycol monoethyl ether (DEGEE), ethylene glycol monomethyl ether (EGME), and ethylene glycol monophenyl ether (EGPhE) into the binary blend, and H_m^E values were obtained for several compositions.

All systems displayed positive excess molar enthalpies at both temperatures, indicating endothermic mixing. The experimental results were examined with several thermodynamic models, namely the R–K equation, NRTL, UNIQUAC, and modified UNIFAC (Dortmund). For the binary mixture, the R–K approach yielded the most satisfactory agreement with experimental data. When considering the ternary mixtures, the ΔH_{123}^E, Eq. (17), and NRTL model proved to be the most suitable for reproducing the experimental measurements. Additional predictions were carried out with NRTL, UNIQUAC, and UNIFAC. Among these, NRTL consistently showed the closest match to experimental values, whereas UNIFAC led to the largest deviations depending on the glycol ether involved.

Supplementary Information The online version contains supplementary material available at https://doi.org/10.1007/s10973-026-15354-1.

Author contributions Khaoula Samadi contributed to writing—original draft, investigation, and formal analysis and provided software; Mohamed Lifi contributed to writing—review and editing the manuscript, investigation, and formal analysis and provided software; Raúl Briones Llorente was involved in investigation and formal analysis; and Fernando Aguilar and Fatima Ezzahrae M'hamdi Alaoui were involved in supervision and validation.

Funding Open access funding provided by FEDER European Funds and the Junta de Castilla y León under the Research and Innovation Strategy for Smart Specialization (RIS3) of Castilla y León 2021-2027. This work was supported by open-access funding provided by UNIVERSIDAD DE BURGOS.

Declarations

Conflict of interest The authors declare that they have no known competing financial interests or personal relationships that could have appeared to influence the work reported in this paper.

References

1. Carvalho PJ, Fonseca CHG, Moita M-LCJ, Santos ÂFS, Coutinho JAP, American Chemical Society (ACS). Thermophysical properties of glycols and glymes. J Chem Eng Data. 2015;60:3721–37. https://doi.org/10.1021/acs.jced.5b00662.
2. Ansari MF, Maurya AK, Kumar A, Elangovan S. Manganese-catalyzed C–C and C–N bond formation with alcohols via borrowing hydrogen or hydrogen auto-transfer. Beilstein J Org Chem. 2024;20:1111–66. https://doi.org/10.3762/bjoc.20.98.
3. Michniewicz N, Muszyński AS, Wrzeszcz W, Czarnecki MA, Golec B, Hawranek JP, et al. Vibrational spectra of liquid 1-propanol. J Mol Struct. 2008;887:180–6. https://doi.org/10.1016/j.molstruc.2008.03.020.
4. Çelebi Y, Cengiz M, Aydın H. Propanol and its blend in diesel engines: an extensive review. J Energy Inst. 2025;120:102047. https://doi.org/10.1016/j.joei.2025.102047.

5. Rajak U, Panchal M, Veza I, Verma TN, Ağbulut Ü. An experimental and simulation study for hydrogen and short-chain alcohol along with diesel fuel on the CRDI engine behaviors. Int J Thermofluids. 2025;26:101149. https://doi.org/10.1016/j.ijft.2025.101149.
6. Sanz LF, González JA, Hevia F, Cobos JC. Vm Measurements for Benzylamine + Heptane or + 1-Alkanol Mixtures at 298.15 K. Application of the Disquac and eras models.
7. Bigi A, Comelli F. Excess molar enthalpies of binary mixtures containing ethylene glycols or poly(ethylene glycols)+ethyl alcohol at 308.15K and atmospheric pressure. Thermochim Acta. 2005;430:191–5. https://doi.org/10.1016/j.tca.2005.01.064.
8. Kozak M, Merkisz J. Oxygenated diesel fuels and their effect on PM emissions. Appl Sci. 2022;12:7709. https://doi.org/10.3390/app12157709.
9. Prausnitz JM. Molecular thermodynamics of fluid-phase equilibria. 3rd ed. Upper Saddle River, N.J: Prentice Hall PTR; 1999.
10. Redlich O, Kister AT. Algebraic representation of thermodynamic properties and the classification of solutions. Ind Eng Chem. 1948;40:345–8. https://doi.org/10.1021/ie50458a036.
11. Abbott MM, Van Ness HC. Vapor-liquid equilibrium: part III. Data reduction with precise expressions for G^E. AIChE J. 1975;21:62–71. https://doi.org/10.1002/aic.690210107.
12. Weidlich U, Gmehling J. A modified UNIFAC model. 1. Prediction of VLE, hE, and .gamma..infin. Ind Eng Chem Res. 1987;26:1372–81. https://doi.org/10.1021/ie00067a018.
13. Abrams DS, Prausnitz JM. Statistical thermodynamics of liquid mixtures: a new expression for the excess Gibbs energy of partly or completely miscible systems. AIChE J. 1975;21:116–28. https://doi.org/10.1002/aic.690210115.
14. Makhlouf H, Muñoz-Rujas N, Aguilar F, Belhachemi B, Montero EA, Bahadur I, et al. Density, speed of sound and refractive index of mixtures containing 2-phenoxyethanol with propanol or butanol at various temperatures. J Chem Thermodyn. 2019;128:394–405. https://doi.org/10.1016/j.jct.2018.08.029.
15. Lifi M, Abala I, Munoz-Rujas N, Aguilar F, Montero EA, Negadi L, et al. Thermophysical properties of binary liquid mixtures of oxygenated compounds: 2-methoxyethanol + alcohols at T = 298.15 K and 313.15 K. J Chem Thermodyn. 2022;164:106593. https://doi.org/10.1016/j.jct.2021.106593.
16. Lifi M, Muñoz-Rujas N, Rubio-Pérez G, Aguilar F, M'hamdi Alaoui FE, American Chemical Society. Measurement of liquid density of mixtures of 1-propanol + 2-(2-methoxyethoxy)ethanol at temperatures from 298.15 to 393.15 K and pressures up to 140 MPa and modeling using PC-SAFT and Peng–Robinson equations of state. J Chem Eng Data. 2024;69:2554–68. https://doi.org/10.1021/acs.jced.4c00232.
17. Lifi M, Lorenzo J, Aguilar F, Muñoz-Rujas N, Montero EA, Chhiti Y, et al. Excess enthalpy, density, speed of sound and refractive index of binary mixtures {2-(2-ethoxyethoxy)ethanol + 1-hexene, or cyclohexane, or methylcyclohexane at (298.15 and 313.15) K: application of the PPR-78 cubic equation of state, NRTL and UNIQUAC models. J Chem Thermodyn. 2021;153:106306. https://doi.org/10.1016/j.jct.2020.106306.
18. Lifi H, Aitbelale R, Lifi M, Muñoz-Rujas N, Ezzahrae M'hamdi AF, Aguilar F. Thermodynamic analysis of excess molar enthalpy dynamics in mixtures containing ethanol, methanol, and alkoxyethanols as biofuels for enhanced combustion performance. J Chem Thermodyn. 2025;201:107406. https://doi.org/10.1016/j.jct.2024.107406.
19. Aguilar F, Alaoui FEM, Alonso-Tristán C, Segovia JJ, Villamañán MA, Montero EA. Excess enthalpies of binary and ternary mixtures containing dibutyl ether, cyclohexane and 1-butanol at 298.15 K. J Chem Eng Data. 2009;54:2341–2. https://doi.org/10.1021/je900560j.
20. European co-operation for Accreditation (EA), expression of the uncertainty of measurement in Calibration, EA-4/02, December 1999.
21. Bevington P, Robinson D. Data reduction and error analysis. Data Reduct Error Anal Phys Sci. 2003; 194–217.
22. Gmehling J, Li J, Schiller M. A modified UNIFAC model. 2. Present parameter matrix and results for different thermodynamic properties. Ind Eng Chem Res. 1993;32:178–93. https://doi.org/10.1021/ie00013a024.
23. Lifi M, Muñoz-Rujas N, Rubio-Pérez G, Aguilar F, M'hamdi Alaoui FE. Measurement of liquid density of mixtures of 1-propanol + 2-(2-methoxyethoxy)ethanol at temperatures from 298.15–393.15 K and pressures up to 140 MPa and modeling using PC-SAFT and Peng–Robinson equations of state. J Chem Eng Data. 2024;69:2554–68. https://doi.org/10.1021/acs.jced.4c00232.
24. Pflug HD, Pope AE, Benson GC. Heats of mixing of normal alcohols at 25 °C. J Chem Eng Data. 1968;13:408–10.
25. Zou X, Zi M, Liu K, Wu T, Chen D. The molecular chain's length effect of alcohol and ether for synergistic enhancement with novel kinetic hydrate inhibitors in hydrate inhibition. Fuel. 2024;371:131987. https://doi.org/10.1016/j.fuel.2024.131987.
26. Chegini FP, Iloukhani H, Khanlarzadeh Kh. The study of thermodynamic properties of diethylene glycol monoethyl ether with 2-alkanols (C3–C7) with use of PFP and ERAS modeling. J Chem Thermodyn. 2025;201:107392. https://doi.org/10.1016/j.jct.2024.107392.
27. Nowok A, Dulski M, Grelska J, Szeremeta AZ, Jurkiewicz K, Grzybowska K, et al. Phenyl ring: a steric hindrance or a source of different hydrogen bonding patterns in self-organizing systems? J Phys Chem Lett. 2021;12:2142–7. https://doi.org/10.1021/acs.jpclett.1c00186.